JCI The Journal of Clinical Investigation

Marburg virus glycoprotein mRNA vaccine is more protective than a virus-like particle-forming mRNA vaccine

Chandru Subramani, … , Andrea Carfi, Alexander Bukreyev

J Clin Invest. 2025. https://doi.org/10.1172/JCI194586.

Research In-Press Preview Infectious disease Virology

Graphical abstract

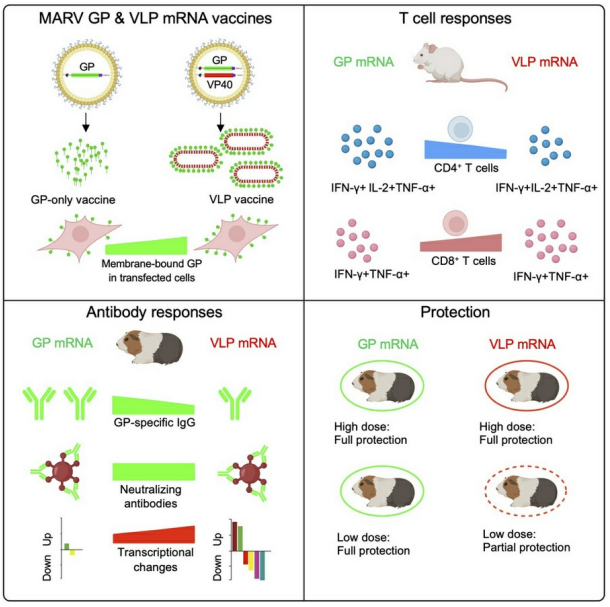

Marburg virus glycoprotein mRNA vaccine is more protective than a virus-like particle-forming mRNA vaccine

Chandru Subramani,[1,2] Michelle N. Meyer,[1,2] Matthew A. Hyde,[3] Margaret E. Comeaux,[3] Haiping Hao,[4] James E. Crowe, Jr,[5,6,7], Vsevolod L. Popov,[1,2], Harshwardhan Thaker,[1] Sunny Himansu,[8] Andrea Carfi,[8*] Alexander Bukreyev[1,2,9,10**]

[1] Department of Pathology, University of Texas Medical Branch at Galveston, Galveston, Texas, USA

[2] Galveston National Laboratory, Galveston, Texas, USA

[3] Animal Resources Center, University of Texas Medical Branch, Galveston, Texas, USA

[4] Department of Biochemistry & Molecular Biology, University of Texas Medical Branch, Galveston, Texas, USA

[5] Vanderbilt Vaccine Center, Vanderbilt University Medical Center, Nashville, TN

[6] Department of Pathology, Microbiology, and Immunology, Vanderbilt University Medical Center, Nashville, Tennessee, USA

[7] Department of Pediatrics (Infectious Diseases), Vanderbilt University Medical Center, Nashville, Tennessee, USA

[8] Moderna Inc., Cambridge, Massachusetts, USA

[9] Department of Microbiology and Immunology, University of Texas Medical Branch, Galveston, Texas, USA

[10] Center for Biodefense and Emerging Viral Infections, University of Texas Medical Branch, Galveston, Texas, USA

Corresponding authors:

Andrea Carfi, Andrea.Carfi@modernatx.com, 325 Binney St, Cambridge, Massachusetts, USA, 02142, Phone: 617-714-6500

Alexander Bukreyev, Alexander.bukreyev@utmb.edu, 301 University Boulevard, University of Texas Medical Branch, Galveston, Texas, USA, 77555-0609, Phone: 409-772-2829

Conflict of interest: SH and AC are employees of Moderna Inc.

ABSTRACT

Although virus-like particle (VLPs) vaccines were shown to be effective against several viruses, their advantage over vaccines which include envelope protein only is not completely clear, particularly for mRNA-encoded VLPs. We conducted a side-by-side comparison of the immunogenicity and protective efficacy of mRNA vaccines encoding for the Marburg virus (MARV) full-length GP delivered alone or as a VLP. Electron microscopy confirmed VLP formation when MARV GP and matrix protein VP40 co-expressed. We vaccinated guinea pigs with a two-component mRNA vaccine encoding for GP and VP40 (VLP) or GP alone. At the highest dose, both vaccines protected fully, although the VLP vaccine elicited a slightly lower humoral response than the GP-only group. However, at low doses, GP-only mRNA conferred 100% protection, whereas the VLP exhibited only partial protection. In mice, VLP mRNA induced a moderate preference for GP-specific $CD8^+$ T cells responses, whereas the GP-only mRNA somewhat favored $CD4^+$ T cell responses. Guinea pig whole blood RNA-seq revealed that the VLP vaccine down-regulated genes associated with various biological and metabolic processes, including the NF-κB signaling pathway, whereas the GP-only vaccine upregulated interferon signaling. Overall, the VLP mRNA vaccine was less immunogenic and protective, whereas the GP-only mRNA vaccine conferred robust protection by as little as one µg dose in guinea pigs.

INTRODUCTION

Marburg virus (MARV) causes a severe disease in humans, characterized by the onset of fever and headache, and can lead to hemorrhagic manifestations with severe bleeding and multiorgan failure, with up to 88% case fatalities (1). MARV is a member of the *Filoviridae* family which includes highly pathogenic viruses Ebola, Sudan, Bungibugyo, and Taï Forest. Two non-endemic countries, Equatorial Guinea and Tanzania, experienced their first-ever outbreak simultaneously in 2023 (2), and new outbreaks occurred in Rwanda in September–November 2024 (3, 4) and in Tanzania in January 2025 (5), highlighting the threat of major outbreaks. There is no approved vaccine against MARV. The virus has a 19.1 kb single-stranded negative-sense RNA genome that encodes seven structural proteins. The glycoprotein (GP) is the sole envelope protein which mediates viral attachment and entry into host cells (6). GP is a key target of antibodies such as MR186 and MR191, shown to be protective in non-human primates (NHPs) (7, 8). Consequently, MARV vaccine development has primarily focused on GP as the immunogen.

Several vaccine platforms, including DNA (9), protein (10), and viral vectors such as adenovirus (Ad) (11), vesicular stomatitis virus (VSV) (12), and modified vaccinia Ankara (MVA) (13), were used for the development of monovalent GP-based vaccines against MARV. Pre-clinical studies also reported multivalent vaccines targeting Ebola, Sudan, Lassa, and Marburg viruses in various combinations (14-16). Chimpanzee adenovirus 3 (cAd3) Marburg GP vaccine induced GP-binding IgG antibodies in 95% of participants and significant GP-specific T-cell responses in phase 1 clinical trial (17). The Ad26.Filo and MVA-BN-Filo multivalent vaccine showed encouraging results in phase 1, but the MARV-specific antibody response was not assessed in the subsequent trials (18-20).

Apart from MARV vaccines solely delivering GP, we and others have reported pre-clinical studies on Marburg virus-like particle (VLP) vaccines, which in addition to GP, includes the matrix protein VP40 with or without the nucleoprotein (NP) (13, 21). A growing body of literature supports the view that VLPs are potent inducers of the immune response by virtue of their structural features, which display highly ordered and repetitive structures that closely resemble the actual viral particles (22). Additionally, the antigenic conformation of viral proteins is retained in VLPs. Most non-enveloped viral capsids self-

assemble to form VLPs without the help of accessory viral proteins (23). All three licensed VLP vaccines against papillomavirus, hepatitis B, and hepatitis E, are comprised of a single protective antibody-inducing antigen (23). However, the external envelope protein of most enveloped viruses requires internal structural proteins, typically the matrix and nucleocapsid proteins, to form VLPs. Hence, VLP vaccines of enveloped viruses carry accessory viral antigens, which can induce non-neutralizing antibodies and possibly protective T-cell responses. These viral accessory antigens may influence immune responses by cooperating or competing with the epitopes of the envelope protein(s) (24, 25). Non-envelope components could also enhance the protection conferred by vaccines based on the envelope protein alone due to formation of VLPs, which are typically highly immunogenic (22). Therefore, it is expected that any immune response induced by the accessory internal protein required for formation of VLPs should contribute the protection, or at a minimum not reduce the envelope-mediated protective response.

MARV and the other members of the *Filoviridae* family, including the Ebola virus, require VP40, for VLP production (26, 27). While the presence of VP40 is an absolute requirement for filovirus VLP formation, some studies have included the NP component in the VLP vaccine. A MARV protein-based VLP vaccine composed of GP, VP40, and NP showed 100% protection in NHPs (21). In addition, we reported that modified vaccinia Ankara (MVA) vectors expressing GP and VP40, the minimum components required for filovirus VLPs, provide complete protection against MARV or Sudan virus in guinea pigs (13, 28). The success of mRNA vaccines in combatting the SARS-CoV-2 pandemic (29, 30) has accelerated the development of mRNA vaccines against an array of viruses such as HIV-I (31), influenza virus (32), respiratory syncytial virus (33), Andes virus (34), Lassa virus (35), and Ebola virus (36), demonstrating the versatility and adaptability of this new vaccine platform. Moreover, two studies have reported VLP mRNA vaccines for HIV-I (31) and SARS-CoV-2 (37). However, it is unclear if the advantages of a VLPs-based vaccine platform can be generalized.

This study aimed to develop a MARV methyl-pseudouridine-modified mRNA vaccine encoding the minimal components for VLP formation and compare its immunogenicity and protective efficacy to a GP-only mRNA vaccine (**Figure 1A**). We used a lethal guinea pig model to show that the GP mRNA vaccine was highly immunogenic and fully protective against MARV infection at a dose as low as 1 μg,

while the VLP-based vaccine was less immunogenic and protective. We demonstrated that GP mRNA induced moderately elevated $CD4^+$ T-cell responses in mice, while VLP mRNA induced moderately increased GP-specific $CD8^+$ T-cell responses. The GP mRNA also induced minimal changes in the guinea pig blood transcriptome after vaccination, while the VLP mRNA downregulated genes associated with cellular and metabolic processes and the NF-κB signaling pathway. These findings shed light on differential immune responses induced by GP and VLP-based mRNA vaccines, which is important for the development of effective vaccines and mitigating their adverse effects.

RESULTS

MARV GP and VP40 mRNA co-expression generates virus-like particles

Several studies have demonstrated that MARV GP and VP40 co-expression generate VLPs (13, 26). Here, we tested the ability of MARV GP and VP40 mRNA co-expression to produce VLPs. To verify the expression of GP and VP40, HEK293T cells were individually transfected or co-transfected with mRNA for 24 h. Western blots on cell lysates (38), 13) revealed the expected molecular weight of GP and VP40 proteins (**Figure 1B**). To confirm VLPs were secreted, supernatants collected 48 h after transfection of HEK293T cellswere clarified by centrifugation, and VLPs were concentrated by ultracentrifugation and analyzed by western blotting (**Figure 1C**).

To determine the optimal GP to VP40 mRNA ratio which promotes high VLP yields and incorporation of GP, a range of GP mRNA concentrations (0.5 to 5 µg) was co-transfected with 1 µg of VP40 mRNA. Intracellular GP levels increased in a GP mRNA concentration-dependent manner, plateauing at 4 µg, while VP40 intracellular levels remained constant. However, the highest incorporation of VP40 into VLPs was acheived at the 1:2 ratio of VP40:GP mRNA, which subsequently decreased as the GP mRNA concentration increased relative to VP40, indicating a reduction in VLP secretion (**Figure 1D–G**). GP incorporation in VLPs was comparable at 1:2 to 1:5 ratios of VP40:GP, with slightly elevated levels observed at a 1:3 ratio. Despite slightly decreased VP40 levels in VLPs, a 1:3 ratio of VP40:GP

was chosen for *in vivo* studies, considering GP is the primary immunogen.

VLPs were visualized using transmission electron microscopy (TEM) on ultrathin sections of HEK293T cells co-expressing GP and VP40 mRNA, or expressing GP mRNA alone (control). VLPs were observed as filamentous structures, with an approximate diameter of 60 nm, and were absent on GP-only-mRNA transfected cells (**Figure 2A and B**). Moreover, negatively stained, sucrose cushion concentrated VLPs formed a club-shaped structure resembling the actual structure of MARV (**Figure 2C**). Immunogold staining with MR235 anti-GP antibody resulted in gold nanoparticle deposition on VLPs, confirming the incorporation of GP proteins (**Figure 2D**).

MARV VP40 increases the levels of membrane-bound GP in mRNA-transfected cells

It was shown that membrane-bound forms of the hemagglutinin (HA) of influenza virus (39) and receptor-binding domain (RBD) of SARS-CoV-2 (40) induce stronger immune responses than their soluble counterparts. MARV VP40 is a key component in virus assembly and budding, which is enriched at the plasma membrane and plays an indispensable role in recruiting and assembling GP and NP to form mature virions (41-43). Therefore, we examined if the expression of GP together with VP40, increased membrane-bound GP. HEK293T or Vero E6 cells were transfected with 300 ng of GP mRNA, or co-transfected with 300 ng of GP mRNA and 100 ng of VP40 mRNA. Twelve and 24 h post-transfection, cells were surface stained with a GP antibody cocktail of MR191, MR228, and MR235 (38), and flow cytometric analysis was performed (**Figure 3A** and **Supplemental Figure 1**). Cells transfected with 300 ng of Andes virus (ANDV) glycoprotein precursor (GPC) mRNA (34) were used as a negative control. Membrane-bound GP was detected in GP and VLP mRNA-transfected cells at 12 and 24 h post-transfection**.** While VP40 did not affect the MFI levels of GP expression, it did significantly increase the percentages of GP-positive cells compared to cells lacking VP40 (**Figure 3, B–E**). Altogether, the flow cytometry data indicates that GP incorporation in cells was improved when delivered in the form of VLPs, which may be a beneficial factor in enhancing GP-mediated immune response.

GP and VLP mRNA vaccines induce a potent GP-binding IgG antibody response in guinea pigs, but their levels for GP mRNA are marginally higher

We assessed the immunogenicity and protective efficacy of GP and VLP mRNA vaccines in Dunkin-Hartley guinea pigs. The VLP-mRNA vaccine was a co-formualtion of the predetermined 1:3 ratio of VP40:GP mRNA in lipid nanoparticles (LNPs). The GP-only mRNA-LNP vaccine was co-formulated with nontranslated Factor IX (NTFIX) mRNA to match the mRNA content delivered to animals. In Study 1, 9-week-old guinea pigs were vaccinated on days 0 and 28 with 10 μg of GP mRNA (GP 7.5 μg + NTFIX 2.5 μg), 10 μg of VLP mRNA (GP 7.5 μg + VP40 2.5 μg), and 40 μg of VLP mRNA (GP 30 μg + VP40 10 μg) (**Figure 4A**).

Four weeks after prime and boost, serum samples were collected to evaluate humoral responses using enzyme-linked immunosorbent assay (ELISA) and a plaque reduction neutralization test (PRNT). Priming induced a comparable, low GP-binding IgG response in all vaccinated groups (**Figure 4, B and C**) which increased strongly following boosting. Interestingly, both 10 and 40 μg of the VLP vaccine elicited marginally lower GP-binding IgG responses than the GP-alone vaccine. Median GP-specific IgG titers were 7,887 (interquartile range (IQR) 5,562–13,153) for GP 10 μg, 3,933 (IQR: 1,487–8,007) for VLP 10 μg, and 5,294 (IQR: 3,428–8,941) for the VLP 40 μg vaccinated group. MARV VP40-binding IgG was detectable in only VLP mRNA vaccinated groups (**Figure 4, D and E**). Therefore, the ELISA data suggest that the GP vaccine elicits slightly elevated GP-binding IgG titers compared to the VLP vaccine.

After priming, not all guinea pigs produced neutralizing antibodies. After boosting, titers were detected in all guinea pigs, albeit at low levels, except for one animal in the VLP 10 μg group (**Figure 4, F and G**). $PRNT_{60}$ median titers were 30 (IQR: 25–114) for GP 10 μg, 34 (IQR: 21–62) for VLP 10 μg, and 55 (IQR: 46–96) for VLP 40 μg mRNA vaccinated groups. However, the difference reached statistical significance only for the VLP 40 μg vaccinated group compared to the NTFIX group; thus, despite the reduced GP IgG response in the VLP 40 μg group, it had slightly elevated levels of neutralizing antibodies compared to GP mRNA. It should be noted that the significant neutralization observed in the 40 μg group reflects its four-fold higher GP mRNA dose rather than vaccine-specific effect. Ten μg doses of GP and VLP mRNA induced equivalent neutralizing antibody responses, suggesting no benefit from the VLP-

formulation. Altogether, the antibody data suggest that GP and VLP mRNA vaccines primarily induce GP-binding IgG responses with limited neutralizing antibodies. Importantly, the GP vaccine induced slightly higher GP-binding IgG titers than the VLP vaccine.

Higher doses of both mRNA vaccines equally protect guinea pigs from death and disease caused by MARV

Four weeks after boosting, guinea pigs were challenged intraperitoneally with 1,000 PFU of the guinea pig-adapted MARV variant Angola. Throughout the infection period, body weight, temperature, and disease scores were recorded daily until day 28 study endpoint. Weight loss, appearance, posture, and neurological symptoms were taken into account in determining the disease score. Disease score 1 indicates that the guinea pig is healthy and shows no signs of illness. Animals which had score of 4 based on clinical signs of disease or >20% weight loss, met the euthasia criteria. Serum was collected every three days through day 12, and upon euthanasia on day 28, blood, liver, spleen, and kidney were collected for viral load quantitation by plaque assay. By day 4 post-infection (dpi), most NTFIX-vaccinated guinea pigs started losing weight, which progressed to 15% below baseline, developed hyperthermia, and demonstrated high disease scores; the guinea pigs succumbed or were found moribund and euthanized on days 7–10 (**Figure 5, A–C**, **Supplemental Figure 2A**). Serum samples from the control group tested positive for infectious virus as early as 3 dpi (**Figure 5, D–G**). Terminal bleed samples of the control group displayed high viral titers. The control group's spleen, liver, and kidney tissue samples also showed high viral load. In contrast, all vaccinated groups showed 100% protection against death and disease, maintained a disease score of 1, normal body temperatures, and weight. The 10 μg VLP group had a marginal but significant increase in body weight compared to the 10 μg GP group on days 10, 11, and 28 ($p < 0.03$, 0.04, and 0.04, respectively). All vaccinated groups had no detectable infectious virus in serum or tissue. The data indicate that both GP and VLP mRNA vaccines confer robust protection against the lethal challenge with MARV despite low or no neutralizing antibodies.

mRNA vaccines elicit potent antibody responses even at the lowest dose, but their levels are slightly elevated in the GP mRNA vaccine group.

To better compare the two vaccine platforms, we tested the GP and VLP mRNA at reduced doses. In Study 2, guinea pigs were vaccinated with GP mRNA at 1 μg and 3 μg doses and VLP mRNA at 1.33 μg (GP 1 μg + VP40 0.33 μg) and 4 μg (GP 3 μg + VP40 1 μg) doses (**Figure 6A**). In addition, the protective doses of GP at 7.5 μg and VLP at 10 μg (GP 7.5 μg + VP40 2.5 μg) mRNA from Study 1 were included again as positive controls. The control group received only phosphate-buffered saline (PBS).

GP-binding IgG antibodies were detectable after priming, even in the 1 μg GP or 1.33 μg VLP mRNA vaccinated group, and their levels increased after boosting. Post-booster serum samples showed that 1 μg and 3 μg of GP mRNA vaccines induced more than three- and two-fold GP IgG levels, respectively, compared to their counterparts in the VLP mRNA group. The median IgG titers were 1,518 (IQR: 783–7,217) for GP 1 μg, 418 (IQR: 356–1,452) for VLP 1.33 μg, 3,477 (IQR: 1,400–6,444) for GP 3 μg and 1,664 (IQR: 1,225–6,666) for VLP 4 μg mRNA vaccinated group (**Figure 6, B–D**). However, 10 μg of VLP mRNA induced nearly three-fold higher IgG levels than 7.5 μg of GP mRNA. The median IgG titers were 4,922 (IQR: 3966-6801) for GP 7.5 μg and 13,207 (IQR: 4685-13207). Except for this outlier, every GP dose in both studies elicited marginally increased GP IgG titers than VLP counterparts. Although the GP IgG titers induced by the identical mRNA doses in both studies differed, statistical analysis found no significant difference (**Supplemental Figure 3, A and B**). As expected, GP-only vaccinated groups had no detectable VP40 IgG antibodies (**Figure 6, E–G**). After boosting, VP40-binding IgG antibodies were detectable in the 4 μg and 10 μg VLP vaccinated groups but not in the 1.33 μg VLP mRNA group. Of note, VP40 IgG levels were slightly higher in the VLP 4 μg vaccinated group than in the 10 μg group. Only the highest doses of GP and VLP mRNA induced neutralizing antibodies after the booster (**Figure 6, H–J**), except for one guinea pig in the 3 μg GP group. These data indicate that even the lowest mRNA doses elicited a robust GP-binding IgG response, but levels were slightly higher in the GP-vaccinated groups than in the VLP mRNA groups.

Only GP mRNA but not VLP confer complete protection at low doses

Four weeks after the boost vaccination, guinea pigs were challenged with the guinea pig-adapted MARV as described in Study 1. The PBS control group developed disease signs and lost body weight up to 15%; they succumbed to infection on days 7–12 (**Figure 7, A–D**). The control group also experienced hyperthermia followed by hypothermia (**Supplemental Figure 2B**). Consistent with clinical signs and high disease scores, serum and tissue samples (spleen, liver, kidney) showed high viral load (**Figure 7, E–H**). On the other hand, all GP mRNA (1, 3, 7.5 μg) and the highest VLP mRNA (10 μg) vaccinated groups survived; all guinea pigs but one in the 3 μg GP group showed no outward signs of illness. The animals maintained normal body temperature **(Supplemental Figure 2C)**, had no or low disease score, gained weight throughout the study, and had no detectable viremia or virus load in organs. In contrast, the 1 μg and 4 μg VLP mRNA vaccinated groups exhibited 80% and 60% protection, respectively. The succumbed guinea pigs lost body weight and had a high disease scores. In addition, all surviving guinea pigs in the 4 μg VLP group developed disease signs with score of 3 before recovering. Viral load analysis revealed that the non-survivor in the 1 μg group had high infectious virus in serum and tissue samples, whereas the two non-survivors in the 4 μg VLP group had no detectable virus.

In the PBS control group, liver tissue sections showed characteristic histopathologic changes, including hepatocellular vacuolation, sinusoidal leukocytosis, apoptosis/necrosis, focal cytoplasmic inclusions, and occasional councilman-like bodies (**Figure 8A**). In contrast, the vaccinated groups displayed normal liver histology except for the non-survivor in the VLP 1 μg group, which displayed histopathologic changes similar to the PBS group (**Figure 8, B and C**). However, non-survivors in the VLP 4 μg group exhibited normal histology with a small amount of glycogen deposition in the liver (**Figure 8D**). Similarly, spleen sections of the control group showed lymphocyte depletion in the white pulp, necrosis, and inflammation in the red pulp with diffuse hemorrhage and tingible-body macrophages (**Figure 8E**). Spleen sections of all vaccinated groups showed normal histology except in the one non-survivor in the VLP 1 μg (**Figure 8, F–H**).

The guinea pig Study 1 demonstrated that 7.5 μg GP and 10 μg VLP mRNA vaccines completely protected against MARV infection. In line with this, the complete protection by high vaccine doses in

Study 2 highlights the reproducibility and robustness of mRNA vaccine-induced protective responses against MARV. These data also show that the lowest GP mRNA vaccine dose tested – 1 µg – provided 100% protection against death and disease caused by a lethal dose of MARV. In contrast, the same dose of GP mRNA vaccine combined with 0.33 µg VP40 mRNA conferred 80% protection. Histology and viral load data demonstrated that the VLP 1 µg guinea pig succumbed due to the infection. The 3 µg GP mRNA group showed 100% protection, but its VLP counterpart showed 60% protection; the lack of detectable viral load and histopathological data indicated that the reduced protection in the 4 µg VLP group was unrelated to viral infection or it could be an unknown VLP vaccine-induced effect.

The VLP mRNA vaccine induces a subtle GP-specific $CD8^+$ T-cell predominance, whereas the GP mRNA induces a modestly skewed $CD4^+$ T-cell response

The low-dose VLP mRNA vaccine conferred incomplete protection compared to the GP-alone mRNA vaccine, which could be attributed to the lower GP-binding IgG antibody titers. We investigated whether these vaccines induce differential $CD8^+$ and $CD4^+$ T-cell responses. To address this, six- to seven-week-old female BALB/c mice were vaccinated on days 0 and 29 with 1 µg of GP mRNA, 1.33 µg of VLP mRNA (GP 1 µg + VP40 0.33 µg) or PBS (control) (**Figure 9A**). Two weeks after boosting, MARV GP-specific $CD4^+$ and $CD8^+$ T cell responses were measured in splenocytes by flow cytometry (**Supplemental Figure 4**). The cells were stimulated with a pool of 15 amino-acid long peptides, which cover the full-length GP of MARV strain Angola with 11 amino acids overlap, and then surface stained for CD4 and CD8 and intracellularly stained for interferon-γ (IFN-γ), interleukin-2 (IL-2), and tumor necrosis factor α (TNF-α). The control cells were mock-stimulated with dimethylsulfoxide (DMSO) (**Figure 9B**)**.** The GP mRNA vaccinated group had significantly more $CD4^+$ T cells positive for IFN-γ, IL-2, or TNF-α, when compared to the control PBS group. Although the VLP-vaccinated group showed GP-specific $CD4^+$ T cell responses, the difference to the PBS-vaccinated control group did not reach statistical significance. Compared to PBS controls, both GP and VLP mRNA groups showed a significant increase in IFN-γ^+ $CD8^+$ T cells, but only VLP mRNA induced a significant increase in TNF-α^+ $CD8^+$ T cells. The GP mRNA vaccine induced more triple-positive $CD4^+$ T cells co-producing IFN-γ, IL-2, and TNF-α, whereas the VLP mRNA vaccine

induced more double-positive $CD8^+$ T cells co-producing IFN-γ and TNF-α (**Figure 9, C and D**). However, none of the $CD4^+$ or $CD8^+$ T cell populations differed significantly when comparing GP and VLP groups directly. Altogether, our data suggest that both mRNA vaccines induced GP-specific T-cell responses with a modest skew towards $CD4^+$ T-cells in the GP mRNA group and $CD8^+$ T-cells in the VLP mRNA group.

The VLP mRNA vaccine but not the GP-only vaccine changes the guinea pig whole blood transcriptome

To understand transcriptional changes in the 4 μg VLP group, which demonstrated reduced survival despite the protection against viral replication, we performed bulk RNA sequencing of guinea pig whole blood for day 54 post-vaccination and day three post-challenge. We included the following groups: PBS control, 3 μg and 7.5 μg of GP mRNA, and 4 μg and 10 μg of VLP mRNA.

Principal component analysis (PCA) of day 54 post-vaccination samples showed that PBS and GP 3 μg groups clustered together, unlike the 4 and 10 μg VLP vaccinated groups **(Figure 10A**). In addition, two samples from the GP 7.5 μg group were also associated with the PBS/GP 3 μg cluster. This suggests that GP mRNA induced minimal changes in the transcriptome, while VLP mRNA induced marked changes. Genes with log2(fold change) >1 and p-value ≤ 0.05 showed that the GP-vaccinated group had no (GP 3 μg) or very low (GP 7.5 μg) differentially expressed genes compared to the PBS group (**Figure 10B**). In contrast, VLP 10 μg and 4 μg had 209 and 16 significantly differentially expressed genes, respectively (**Supplemental Data 1**).

Functional enrichment analysis showed the upregulation of reactome terms for interferon (IFN) signaling in the GP 7.5 μg group (**Figure 10C**). However, the VLP 10 μg group exhibited down-regulated Gene Onthology (GO) terms for biological and metabolic processes, including the NF-kappa B signaling pathway and post-transcriptional silencing by small RNAs; the majority of these down-regulated genes interact with each other and form a highly connected protein-protein interaction network (**Supplemental Figure 5**). In addition, genes involved in the mitochondrial respiratory chain complex were upregulated (**Supplemental Data 1**). Surprisingly, the comparison of VLP 10 μg versus VLP 4 μg showed down-regulation of natural killer cell-mediated cytotoxicity, B-cell receptor signaling, and NF-kappa B pathways.

A closer look at the gene list revealed that the VLP 10 µg group had overlapping genes with VLP 4 µg and GP 7.5 µg groups (**Figure 10, D and E**). Among overlapped genes, we found that GP 7.5 µg and VLP 10 µg mRNA commonly upregulated immune-related genes (**Supplemental Table 1**), HECT and RLD domain containing E3 ubiquitin-protein ligase (*HERC5*), cyclin D1 binding protein 1 (*CCNDBP1*) and interferon-induced protein with tetratricopeptide repeats 1B (*IFIT1B*) (44-46), which were not induced in the VLP 4 µg group. Interestingly, both VLP doses showed upregulated S100 family protein linked to poor prognosis in Ebola virus disease (47) and COVID-19 (48). Overall, the data suggest that GP mRNA induced a minimal effect on the blood transcriptome, whereas VLP mRNA induced more changes. In addition, the high-dose VLP vaccine downregulated genes involved in immune response.

Next, we characterized the differential gene expression of GP and VLP mRNA vaccinated groups in day 3 post-challenge blood samples. PCA indicated that the PBS group separated from all vaccinated groups (**Figure 11A**). Vaccinated groups showed downregulation of 84, 99, 178, and 111 genes in GP 3 µg, GP 7.5 µg, VLP 4 µg and VLP 10 µg vaccinated groups, respectively, as compared to the PBS control (**Figure 11B** and **Supplemental Data 2**) with 45 overlapping genes (**Figure 11C**). These 45 genes enriched for viral immune response and cytokine signaling terms/pathways (**Figure 11D**). These include pathways/signaling associated with TLR, NLR, IFN, complement ,and apoptosis (**Figure 11E**). This demonstrates that vaccinated groups had reduced levels of immune response pathways due to vaccine-mediated protective effects. Of note, the VLP 4 µg group had 71 unique downregulated genes. The analysis of these unique genes did not indicate any pathways correlated with the reduced protection. However, it is tempting to speculate that the down-regulation of a distinct set of genes in the VLP 4 µg group is likely to be associated with the reduced protection in this group. Lastly, comparing VLP 10 µg versus VLP 4 µg showed downregulation of immunoglobulin receptor binding genes. These data suggest that unprotected control guinea pigs had exaggerated immune responses upon MARV infection, characterized by upregulation genes involved in cytokine signaling, whereas vaccinated guinea pigs showed reduced expression of these genes due to vaccine-mediated protective effects.

DISCUSSION

In this study, we developed and assessed the protective efficacy of mRNA vaccines against MARV and addressed whether the MARV VLP vaccine provides an added advantage over the GP-only vaccine. Previous studies showed that protein- or viral vector-derived MARV VLP vaccines were protective in small animals and NHPs, but lacked GP-only control and dose-ranging data, making it unclear whether the VLP vaccine had an edge over the GP vaccine (13, 21). The minimal component MARV strain Musoke VLP vaccine derived from cell culture showed complete protection against challenge with MARV after three intramuscular injections, each consisting of 50 µg dose in guinea pigs and 1 mg dose in NHPs (21). This study provides a more comprehensive understanding of the efficacy of GP and VLP vaccines against MARV. Our side-by-side comparison of VLP and GP groups showed that the VLP vaccine failed to protect guinea pigs at low doses, whereas the GP-alone vaccine displayed 100% protection even at the lowest dose. In addition, our study provides supporting evidence as to why VLP failed to protect.

First, GP-specific binding IgG levels were moderately reduced in the VLP-vaccinated group. The available NHP data indicate that GP-binding IgG levels correlate with protection (11, 49). In line with this, our data also showed that mRNA vaccines conferred complete protection despite no or low detectable neutralizing antibodies, suggesting that Fc-mediated response or alternative antiviral mechanisms mediated by antibodies could play a role in protection (13, 50, 51). Therefore, the reduced protection in the VLP-vaccinated group could be due to reduced levels of GP-binding IgG. Although we reasoned that the reduced GP-binding IgG titers were one of the contributing factors, we could not establish the minimum level of antibodies required for protection due to the modest differences in either GP- or VP40-binding titers, or neutralizing antibody titers between survivors and non-survivors (**Supplemental Tables 2 and 3**). VLP-vaccinated guinea pigs indeed had two- to three-fold reduced median titers of GP-binding IgG at low doses, compared to the GP group; however, within the VLP group, there was no difference in antibody titers between survivors and non-survivors. In the same way, their VP40-specific IgG levels did not correlate with survival, and the majority of them did not elicit virus-neutralizing antibodies.

The role of T-cell immunity in MARV GP-induced protective responses is not completely understood. However, irrespective of a vaccine platform, most GP vaccines have been shown to induce predominantly $CD4^+$ T-cell responses and less $CD8^+$ T-cell responses. ChAdOx1-vectored GP in mice (16), VSV-vectored (52) and DNA encoding GP (53) in NHP, cAd3-vectored GP (17) and DNA encoding GP (9) in phase I clinical trials have reported induction of dominant $CD4^+$ T-cell responses and less frequent $CD8^+$ T-cell responses. Conversely, recombinant Ad5-vectored GP is the only vaccine shown to induce cellular immune response with skewing toward $CD8^+$ T-cells (53). Moreover, analysis of the T-cell immune response from MARV infection survivors showed the development of multifunctional $CD4^+$ T-cell responses expressing IFN-γ and IL-2 with limited $CD8^+$ T-cell responses (54). In line with this data, our mouse study showed that the VLP vaccine elicited moderately elevated $CD8^+$ T-cell responses, whereas the GP vaccine induced $CD4^+$ T-cell responses. Although both vaccines induced $CD4^+$ T-cell responses, the GP-vaccinated group had increased activated $CD4^+$ T-cells co-expressing IFN-γ, IL-2, and TNF-α in contrast to the VLP-vaccinated group, which had slightly more $CD8^+$ T-cells double-positive for IFN-γ and TNF-α. Our data indicate that multi-functional $CD4^+$ T cell response could be associated with protection.

RNA-seq of guinea pig whole blood at day 54 post-vaccination indicated that the VLP mRNA vaccine at 10 μg dose affected gene expression associated with various metabolic and cellular processes. Specifically, genes associated with RISC complex assembly, pre-miRNA processing, RNA secondary structure unwinding, and histone H3-K4 methylation were downregulated. Incidentally, Ebola virus VP30, VP35, and VP40 have been shown to suppress RNA silencing to antagonize RNAi-dependent antiviral immunity (55). In addition, several respiratory chain complex genes were upregulated. Intriguingly, the 10 μg dose of VLPs,compared to the 4 μg dose, induced down-regulation of natural killer cell-mediated cytotoxicity, B-cell receptor signaling, and NF-kappa B pathways. In contrast, GP vaccination induced no changes in the transcriptome in the 3 μg group, and few genes related to type I interferon (IFN-I) signaling were upregulated in the GP 7.5 μg group. Together, the transcriptome data suggest that VP40 induced substantial changes in the gene expression of the whole blood. Moreover, MARV VP40 has been shown to antagonize IFN-I signaling by inhibiting the phosphorylation of Janus kinases and STAT proteins in response to IFN-I and type II interferon, as well

366 as interleukin 6 (56, 57). Hence, VP40 could exhibit some indirect effects on host immune cells, thereby
367 affecting the immune response to GP.

368 It is well-known that innate immune signaling is the first line of defence against viruses, including
369 MARV (12, 58, 59). In line with this, after the challenge, unvaccinated guinea pigs showed upregulation
370 of genes involved in pattern recognition receptors (TLR4, NLRC5), IFN-I pathway (IFIT1B, IFIH1,
371 IFGGB1, IFGGC3, OAS1, OAS3, STING1), complement pathway (C1QC, C1QA), apoptosis pathway
372 (CASP10) and EIF2AK2, double-stranded RNA-activated protein kinase. However, vaccinated animals
373 had reduced levels of these transcripts, indicating vaccine-mediated protective effects upon MARV
374 infection. Interestingly, in the VLP 4 µg vaccinated group, which had two non-survivors, 178 genes were
375 downregulated; this is nearly two-fold higher than in the other vaccinated groups. Hence, it is impossible
376 to rule out that VP40-mediated immunosuppressive effects could be the culprit behind the reduced
377 survival of the 4 µg VLP mRNA group despite showing protection from viral infection. Further *in vitro* and
378 *in vivo* studies are needed to understand how VP40 modulates host cell function.

379 The results from this study raise an important question: are the VP40-mediated adverse effects
380 restricted to MARV or does it apply to other viruses in the filovirus family, such as Ebola virus, even
381 though IFN-I antagonism of Ebola virus is associated with VP35 and VP24 (60) rather than VP40? One
382 NHP study indirectly suggested that VP40-mediated effects could also be extended to Ebola virus, in
383 which the EBOV GP-VP40 VLP (VLP two-component) protein-derived vaccine was tested with the dose
384 range of 25 µg to 3 mg in NHPs (61). The vaccine demonstrated only partial protection even at the highest
385 3 mg dose; survivors had GPΔTM titers >1,400 AU/ml and GPΔmuc titers >1,900 AU/ml, whereas most
386 non-survivors fell below these thresholds. In contrast, NHPs receiving a three-component VLP (with NP
387 also included) or an Ad-GP vaccine achieved GP titers similar to those of non-survivors of EBOV two-
388 component VLP and survived with no symptoms. The authors concluded that the two-component VLP
389 vaccine requires a significantly higher GP antibody threshold for protection than the Ad-GP or triple-
390 component VLP vaccine. In line with this, it is possible that the MARV VLP vaccine may also require a
391 higher GP-antibody threshold for protection than the GP-alone vaccine. Moreover, several other vaccine
392 platforms have shown that GP-only vaccines confer complete protection to NHPs (11, 52, 62). Therefore,

393 it is tempting to speculate that the reduced protection by the Ebola VLP vaccine could be due to VP40-
394 mediated effects. More studies are warranted to reproduce VP40-induced adverse effects and to
395 elucidate the mechanisms by which VP40 modulates host immunity.

396 While mRNA-LNP vaccine technology is now well-established for single-component vaccines, its
397 application to VLP vaccines is still in exploratory stages. Although it was successfully tested for SARS-
398 CoV-2 (37, 63) and HIV-1 (31, 63) in pre-clinical studies, mRNA-derived VLP vaccine needs more studies
399 to match gold-standard protein-derived VLP vaccines. Unlike single-component or bivalent mRNA
400 vaccines, which require only efficient translation of one or two proteins, the VLP mRNA vaccine must
401 accomplish a balanced co-expression of two or more proteins, enrichment at the plasma membrane,
402 assembly, and VLP release. In contrast, protein-derived VLP vaccines are fully assembled and readily
403 accessable to immune cells. Although our *in vitro* data demonstrated VLP assembly and release by
404 mRNA, predicting and demonstrating *in vivo* VLP assembly remains challenging. This is particularly
405 relevant because our study is the first to show reduced immunogenicity and protective efficacy of a VLP
406 mRNA vaccine as compared to an envelope protein only vaccine. Further studies are needed to compare
407 VLP mRNA with protein-derived vaccines to ensure that the *in vivo* assembly bottleneck does not impair
408 the vaccine efficacy.

409 The study's major limitation is VP40's multifaceted role in MARV VLP formation, which
410 complicates the understanding of its specific impact on GP-mediated immune modulation. VP40
411 oligomerizes at the inner plasma membrane to form lattice structures and recruits GP, NP, and accessory
412 components to budding sites, facilitating MARV assembly and release (41-43). In line with this well-
413 established data, our *in vitro* results showed enhanced surface GP expression, VLP assembly, and
414 release in the presence of VP40. However, the VLP vaccine did not induce enhanced antibody response
415 and displayed reduced protection. It should be emphasized that GP expressed alone is partly surface-
416 expressed and secreted; in contrast, GP co-expression with VP40 enhances surface expression and is
417 released as VLP, altering the balance between intracellular, surface-bound, and extracellular GP. Despite
418 the fact that we administered equal amounts of GP-encoding mRNA in guinea pigs, the resulting GP
419 could be distributed differently across the cell, complicating the direct comparison of these vaccine

formulations. Although the surface GP expression we measured could represent a transient intermediate step, and surface-expressed GP could ultimately become a part of VLP, it is noteworthy that mRNA-derived membrane-bound immunogens lower the activation threshold for germline-targeting antibody responses (64). Therefore, the reduced protection by VLP may stem from altered GP distribution or VP40's direct immunomodulatory effects. Further studies are needed to dissect VP40's specific immunomodulatory roles and to clarify how differential GP localization influences protective immunity.

In summary, we developed mRNA-based vaccines against MARV and demonstrated excellent immunogenicity and protection for the GP-only vaccine. However, the MARV VLP vaccine did not exhibit enhanced immune response and protection compared to the GP-only vaccine suggesting that the presence of VP40 or the assembly of the vaccine components in VLPs has reduced the GP-mediated immune response.

METHODS

Sex as a biological variable. Our study exclusively examined female guinea pigs and mice. There are no indications of any significant difference between male and female guinea pigs and mice in immune response to mRNA vaccines and between male and female guinea pigs in susceptibility to Marburg virus. Selection of female guinea pigs was also related to limited space in BSL-4 containment.

Development of the mRNA vaccines. mRNA vaccine encoding GP and VP40 for MARV were synthesized *in vitro* using an optimized T7 RNA polymerase-mediated transcription reaction and formulated in lipid nanoparticles (LNPs) as described previously (37).

Confirmation of GP and VP40 protein expression by western blotting. HEK293T cells with 70–80% confluence were individually or co-transfected with 500 ng of GP and VP40 mRNA in 24-well plates using the TransIT-mRNA Transfection Kit (Mirus Bio) following the manufacturer's guidelines. At 24 h post-

transfection, cells were lysed in cell lysis buffer (Cell Signaling Technology, #9803) with a protease inhibitor. Proteins were quantified using the BCA Protein Assay kit (Pierce, #23227) and equalized. Proteins were separated by NuPAGE Bis-Tris Mini Protein Gels (Invitrogen, NP0322BOX) and transferred to nitrocellulose membrane using iBlot 2 Dry Blotting System (Invitrogen, #IB23001). Then, blots were incubated with a blocking buffer (LI-COR, #927-70001) and primary and secondary antibodies. Human monoclonal antibody MR235 (38) and mouse monoclonal antibody 6B1 (IBT Bioservices, #0203-016) were used to detect GP and VP40 proteins, respectively. Fluorescently labelled secondary antibodies (LI-COR) were used and visualized using Odyssey Fc OFC-1130 (LI-COR). Fluorescent intensity of protein bands were quantified using the in-built software of Odyssey. For optimizing GP and VP40 mRNA ratio, 0.5, 1, 2, 3, 4, and 5 µg of GP mRNA were co-transfected with 1 µg of VP40 mRNA for 48 h in HEK293T cells in 100 mm plates. VLPs were purified from culture supernatant as described below. Cell lysates and purified VLPs were analyzed using western blotting.

Purification of virus-like particles from culture supernatant. As described above, 10 µg GP and VP40 mRNA were transfected in HEK293T cells in a T-75 flask. At 48 h post-transfection, the supernatants were clarified by centrifugation at 1,700 g for 10 min at 4°C. The clarified supernatants were layered over the 25% sucrose and centrifuged in a SW32 rotor of Beckman Coulter Optima L-90K ultracentrifuge for 2 h at 27,000 rpm at 4°C. The pellets were dissolved in STE buffer (Fisher Bioreagents, #BP2479-1) and analyzed by western blotting and TEM.

Electron microscopy of Marburg virus-like particles. HEK293T cells were transfected with 20 µg of GP or GP and VP40 mRNA in two T-75 flasks to prepare ultrathin sections for TEM imaging. The cells were fixed in a fixative buffer containing 2.5% formaldehyde, 0.1% glutaraldehyde, 0.01% picric acid (trinitrophenol), 0.03% $CaCl_2$, 0.05 M cacodylate buffer pH 7.3 – 7.4 for 2–3 h at room temperature. Then, cells were washed thrice with 0.1 M cacodylate buffer each for 10 min at room temperature, followed by incubation with 2% uranyl acetate for 20 min at 60°C with subsequent incubation with 50%, 75%, 95%, and 100% ethanol. Then, samples were infiltered with propylene oxide and embedded in Poly/Bed 812

resin (Polysciences). Finally, blocks were trimmed, sectioned, and visualized under a JEM-1400 electron microscope (JEOL, Ltd). For negative staining of VLPs, 10 µl of purified VLPs were applied on nickel grids and incubated for 10 min, followed by 2% aqueous uranyl acetate treatment for 1 min and then observed under the electron microscope. For immunogold staining, VLPs were applied on nickel grids, followed by incubation with MR235 human monoclonal antibody and 6 nm colloidal gold goat anti-human antibody (Jackson ImmunoResearch Laboratories). Then, grids were fixed in 2% aqueous glutaraldehyde, stained with 2% aqueous uranyl acetate, and observed under the electron microscope.

Surface staining of mRNA transfected HEK293T and Vero E6 cells. HEK293T and Vero E6 cells with 70–80% confluence were individually transfected with 300 ng of GP, 300 ng of Andes virus glycoprotein precursor (GPC) or co-transfected with 300 ng of GP and 100 ng of VP40 mRNA in 24-well plates using the TransIT-mRNA Transfection Kit (Mirus Bio) following the manufacturer's guidelines. At 12 h and 24 h post-transfection, cells were detached using a cell dissociation solution non-enzymatic (Sigma-Aldrich, #C5914-100ML) and stained with a GP antibody cocktail of MR191, MR228, and MR235 (38) and followed by staining with Alexa Flour 488 goat anti-human IgG (Invitrogen, #A11013). The cells were analyzed using Accuri C6 Plus (BD Biosciences), and the data were analyzed using FlowJo v10.9.0.

Viruses. Wild-type MARV strain Angola was used for PRNT assays and guinea pig-adapted MARV strain Angola was used for animal studies. MARV strain 200501379 Angola was isolated during the outbreak in 2005 in Angola (65) and passaged three times in Vero-E6 cells. The guinea pig-adapted Angola strain of MARV used for infection of guinea pigs was provided by Dr. G. Kobinger (while at the Canadian National Microbiology Laboratory). This virus was isolated originally from a patient in Angola, passaged once in Vero-E6 cells, passaged eight times in Hartley guinea pigs using liver and spleen homogenates, once in Vero PP cells, and once in Vero E6 cells for stock production.

Animal and biocontainment work. All the work with infectious MARV was carried out in BSL-4 facilities at Galveston National Laboratory, UTMB. MARV-infected tissue and blood samples were inactivated by

formalin and Trizol for downstream processing, following the UTMB Institutional Biosafety Committee-approved inactivation protocols. Similarly, plaque assay plates were also inactivated using an approved inactivation protocol.

Guinea pig study 1. Five-week-old female outbred Hartley guinea pigs were acquired from Charles River Laboratories. Guinea pigs were anesthetized with 5% isoflurane for vaccinations, blood collection, and virus challenge. On days 0 and 28, guinea pigs received prime and boost doses via the intramuscular route in the left leg in 100 µl volume. Vaccines were diluted in PBS before administration. The doses were 10 µg of GP mRNA (GP 7.5 µg + NTFIX 2.5 µg), 10 µg of VLP mRNA (GP 7.5 µg + VP40 2.5 µg), 40 µg of VLP mRNA (GP 30 µg + VP40 10 µg) vaccines and 40 µg of NTFIX mRNA. Blood was collected on days 27 and 54 post-vaccination. On day 56, guinea pigs were challenged with 1,000 PFU of guinea pig-adapted MARV strain Angola intraperitoneally. Post-challenge guinea pigs were monitored one to three times per day, depending on the disease score. Temperature, weight, and disease scores were documented. Serum samples were collected post-infection on days 3, 6, 9, and 12. Additionally, terminal serum and tissue samples (liver, spleen, and kidney) were collected on day 28 or when the guinea pig succumbed to infection.

Guinea pig study 2. The study was conducted similarly to study 1 with the following changes. Guinea pigs received a booster dose on day 29. Post-prime vaccination blood was collected on day 29. The doses were: GP mRNA 1, 3 and 7.5 µg, VLP mRNA 1.33 µg (GP 1 µg + VP40 0.33 µg), VLP mRNA 4 µg (GP 3 µg + VP40 1 µg) and 10 µg (GP 7.5 µg + VP40 2.5 µg). The control group received PBS.

Mouse study. Six- to seven-week-old female BALB/c were acquired from Charles River Laboratories. Mice were anesthetized with 5% isoflurane for vaccinations and blood collection. On days 0 and 29, mice received prime and boost doses via the intramuscular route in the left leg in 50 µl volume. Vaccines were diluted in PBS before administration. The doses were GP mRNA 1 µg and VLP mRNA 1.33 µg (GP 1 µg + VP40 0.33 µg). On day 42, mice were euthanized, and their spleens were collected.

Liver and spleen histopathology. Organs obtained at necropsy were fixed in neutral buffered formalin and submitted to the institutional research histology service of the biorepository core for processing. Tissue cassettes were processed on a Sakura VIP6 tissue processor for routine histology (total run time of 28.5 h). Embedding of tissue blocks was performed on an Epredia Histostar Embedding Station. Blocks were sectioned at 4 μm using the ThermoScientifc Microm-HM315 microtome. Finally, a standard staining protocol on the Sakura Tissue-Tek Prisma tissue stainer was used to stain the tissues with haematoxylin and eosin.

Bulk RNA sequencing and data analysis. RNA sample quality was assessed using Agilent Bioanalyzer RNA Pico Chips (Agilent). RNAseq libraries were then prepared using NEBNext PolyA module (#7490) and Ultra II Directional RNA library preparation kit (NEB, #7760) following manufacturer's recommended procedure. The resulting libraries were run on Agilent Bioanalyzer High Sensitivity DNA Chips for size and quantified using qPCR. Sequencing was carried out on Element Biosciences Aviti sequencer (Element Biosciences) using paired end 150 bp parameter to a sequencing depth of about 40 million paired reads per sample. The reads were quality filtered and trimmed for adapter sequence using Trimmomatic-0.39 (66) and aligned to guinea pig reference genome Cavpor3.0.112 using STAR 2.7.11a (67). Differential expression was performed using Bioconductor DESeq2 package (68), and functional enrichment analysis was performed using STRING version 12.0 (69). Overlapping genes were analyzed using InteractiVenn (70).

Data availability. All source data values are provided in the Supporting Data Values file. RNA-Seq data were deposited in the NCBI’s Gene Expression Omnibus database and are accessible through GEO Series accession number GSE298124.

Statistical analysis. Statistical analysis was performed using GraphPad Prism 10.2.3. Data were presented as median and interquartile ranges or individual values. The Log Rank (Mantel-Cox) test was used to analyze the survival data. Kruskal–Wallis analysis followed by Dunn's Multiple Comparison Test

or Two-Way ANOVA Analysis followed by Dunn's Multiple Comparison Test were employed for group comparisons.

Study approval. All animal experiments were conducted in compliance with the regulations set out by the University of Texas Medical Branch's Institutional Animal Care and Use Committee (IACUC).

ACKNOWLEDGEMENTS

We thank UTMB Animal Resources Center members for supporting the guinea pig and mice experiments at Galveston National Laboratory BSL-2 and BSL-4 facilities. We thank the UTMB Next Generation Sequencing Core Facility for performing bulk RNA-seq and data analysis and the UTMB Pathology Imaging Core Laboratory for processing samples for histopathology. We also thank Meredith Weglarz and the UTMB Flow Cytometry and Cell Sorting Core Lab for assistance with flow cytometry data acquisition and the UTMB Electron Microscopy Laboratory in the Department of Pathology for processing samples and TEM imaging. We are grateful to the Bukreyev lab members for their support and encouragement. Figure 1A, 4A, 6A and 9A were created with BioRender. This study was supported by a grant from the National Institute of Allergy and Infectious Disease 1 R01 AI41661-01 (to A. B.).

REFERENCES

1. Srivastava S, Sharma D, Kumar S, Sharma A, Rijal R, Asija A, et al. Emergence of Marburg virus: a global perspective on fatal outbreaks and clinical challenges. *Front Microbiol.* 2023;14:1239079.
2. Sibomana O, and Kubwimana E. First-ever Marburg virus disease outbreak in Equatorial Guinea and Tanzania: An imminent crisis in West and East Africa. *Immun Inflamm Dis.* 2023;11(8):e980.
3. Sidik S. Lethal Marburg virus is on the rise in Rwanda: why scientists are worried. *Nature.*

2024;634(8034):522-3.

4. CDC. Marburg Outbreak in Rwanda Situation Summary. https://www.cdc.gov/marburg/situation-summary/index.html (2024).

5. WHO. Marburg viruse disease – United Republic of Tanzania. 2025. https://www.who.int/emergencies/disease-outbreak-news/item/2025-DON559

6. Carette JE, Raaben M, Wong AC, Herbert AS, Obernosterer G, Mulherkar N, et al. Ebola virus entry requires the cholesterol transporter Niemann-Pick C1. *Nature.* 2011;477(7364):340-3.

7. Cross RW, Bornholdt ZA, Prasad AN, Borisevich V, Agans KN, Deer DJ, et al. Combination therapy protects macaques against advanced Marburg virus disease. *Nat Commun.* 2021;12(1):1891.

8. Mire CE, Geisbert JB, Borisevich V, Fenton KA, Agans KN, Flyak AI, et al. Therapeutic treatment of Marburg and Ravn virus infection in nonhuman primates with a human monoclonal antibody. *Sci Transl Med.* 2017;9(384): eaai8711.

9. Sarwar UN, Costner P, Enama ME, Berkowitz N, Hu Z, Hendel CS, et al. Safety and immunogenicity of DNA vaccines encoding Ebolavirus and Marburgvirus wild-type glycoproteins in a phase I clinical trial. *J Infect Dis.* 2015;211(4):549-57.

10. Lehrer AT, Chuang E, Namekar M, Williams CA, Wong TAS, Lieberman MM, et al. Recombinant Protein Filovirus Vaccines Protect Cynomolgus Macaques From Ebola, Sudan, and Marburg Viruses. *Front Immunol.* 2021;12:703986.

11. Hunegnaw R, Honko AN, Wang L, Carr D, Murray T, Shi W, et al. A single-shot ChAd3-MARV vaccine confers rapid and durable protection against Marburg virus in nonhuman primates. *Sci Transl Med.* 2022;14(675):eabq6364.

12. Marzi A, Menicucci AR, Engelmann F, Callison J, Horne EJ, Feldmann F, et al. Protection Against Marburg Virus Using a Recombinant VSV-Vaccine Depends on T and B Cell Activation. *Front Immunol.* 2018;9:3071.

13. Malherbe DC, Domi A, Hauser MJ, Meyer M, Gunn BM, Alter G, et al. Modified vaccinia Ankara vaccine expressing Marburg virus-like particles protects guinea pigs from lethal Marburg virus

609 infection. *NPJ Vaccines.* 2020;5(1):78.
610 14. Swenson DL, Wang D, Luo M, Warfield KL, Woraratanadharm J, Holman DH, et al. Vaccine to
611 confer to nonhuman primates complete protection against multistrain Ebola and Marburg virus
612 infections. *Clin Vaccine Immunol.* 2008;15(3):460-7.
613 15. Tiemessen MM, Solforosi L, Dekking L, Czapska-Casey D, Serroyen J, Sullivan NJ, et al.
614 Protection against Marburg Virus and Sudan Virus in NHP by an Adenovector-Based Trivalent
615 Vaccine Regimen Is Correlated to Humoral Immune Response Levels. *Vaccines (Basel).*
616 2022;10(8):1263.
617 16. Flaxman A, Sebastian S, Appelberg S, Cha KM, Ulaszewska M, Purushotham J, et al. Potent
618 immunogenicity and protective efficacy of a multi-pathogen vaccination targeting Ebola, Sudan,
619 Marburg and Lassa viruse. *PLoS Pathog.* 2024;20(6):e1012262.
620 17. Hamer MJ, Houser KV, Hofstetter AR, Ortega-Villa AM, Lee C, Preston A, et al. Safety, tolerability,
621 and immunogenicity of the chimpanzee adenovirus type 3-vectored Marburg virus (cAd3-
622 Marburg) vaccine in healthy adults in the USA: a first-in-human, phase 1, open-label, dose-
623 escalation trial. *Lancet.* 2023;401(10373):294-302.
624 18. Lariviere Y, Matuvanga TZ, Osang'ir BI, Milolo S, Meta R, Kimbulu P, et al. Ad26.ZEBOV, MVA-
625 BN-Filo Ebola virus disease vaccine regimen plus Ad26.ZEBOV booster at 1 year versus 2 years
626 in health-care and front-line workers in the Democratic Republic of the Congo: secondary and
627 exploratory outcomes of an open-label, randomised, phase 2 trial. *Lancet Infect Dis.*
628 2024;24(7):746-59.
629 19. Goldstein N, McLean C, Gaddah A, Doua J, Keshinro B, Bus-Jacobs L, et al. Lot-to-lot
630 consistency, immunogenicity, and safety of the Ad26.ZEBOV, MVA-BN-Filo Ebola virus vaccine
631 regimen: A phase 3, randomized, double-blind, placebo-controlled trial. *Hum Vaccin Immunother.*
632 2024;20(1):2327747.
633 20. Bockstal V, Shukarev G, McLean C, Goldstein N, Bart S, Gaddah A, et al. First-in-human study to
634 evaluate safety, tolerability, and immunogenicity of heterologous regimens using the multivalent
635 filovirus vaccines Ad26.Filo and MVA-BN-Filo administered in different sequences and schedules:

636 A randomized, controlled study. *PLoS One.* 2022;17(10):e0274906.
637 21. Swenson DL, Warfield KL, Larsen T, Alves DA, Coberley SS, and Bavari S. Monovalent virus-like
638 particle vaccine protects guinea pigs and nonhuman primates against infection with multiple
639 Marburg viruses. *Expert Rev Vaccines.* 2008;7(4):417-29.
640 22. Mohsen MO, and Bachmann MF. Virus-like particle vaccinology, from bench to bedside. *Cell Mol*
641 *Immunol.* 2022;19(9):993-1011.
642 23. Kheirvari M, Liu H, and Tumban E. Virus-like Particle Vaccines and Platforms for Vaccine
643 Development. *Viruses.* 2023;15(5):1109.
644 24. Abt ER, Lam AK, Noguchi M, Rashid K, McLaughlin J, Teng PL, et al. Staggered immunization
645 with mRNA vaccines encoding SARS-CoV-2 polymerase or spike antigens broadens the T cell
646 epitope repertoire. *Proc Natl Acad Sci U S A.* 2024;121(49):e2406332121.
647 25. Kallas EG, Grunenberg NA, Yu C, Manso B, Pantaleo G, Casapia M, et al. Antigenic competition
648 in CD4(+) T cell responses in a randomized, multicenter, double-blind clinical HIV vaccine trial.
649 *Sci Transl Med.* 2019;11(519):eaaw1673.
650 26. Swenson DL, Warfield KL, Kuehl K, Larsen T, Hevey MC, Schmaljohn A, et al. Generation of
651 Marburg virus-like particles by co-expression of glycoprotein and matrix protein. *FEMS Immunol*
652 *Med Microbiol.* 2004;40(1):27-31.
653 27. Wan W, Clarke M, Norris MJ, Kolesnikova L, Koehler A, Bornholdt ZA, et al. Ebola and Marburg
654 virus matrix layers are locally ordered assemblies of VP40 dimers. *Elife.* 2020;9: e59225.
655 28. Malherbe DC, Domi A, Hauser MJ, Atyeo C, Fischinger S, Hyde MA, et al. A single immunization
656 with a modified vaccinia Ankara vectored vaccine producing Sudan virus-like particles protects
657 from lethal infection. *NPJ Vaccines.* 2022;7(1):83.
658 29. Baden LR, El Sahly HM, Essink B, Kotloff K, Frey S, Novak R, et al. Efficacy and Safety of the
659 mRNA-1273 SARS-CoV-2 Vaccine. *N Engl J Med.* 2021;384(5):403-16.
660 30. Polack FP, Thomas SJ, Kitchin N, Absalon J, Gurtman A, Lockhart S, et al. Safety and Efficacy of
661 the BNT162b2 mRNA Covid-19 Vaccine. *N Engl J Med.* 2020;383(27):2603-15.
662 31. Zhang P, Narayanan E, Liu Q, Tsybovsky Y, Boswell K, Ding S, et al. A multiclade env-gag VLP

mRNA vaccine elicits tier-2 HIV-1-neutralizing antibodies and reduces the risk of heterologous SHIV infection in macaques. *Nat Med.* 2021;27(12):2234-45.

32. Kackos CM, DeBeauchamp J, Davitt CJH, Lonzaric J, Sealy RE, Hurwitz JL, et al. Seasonal quadrivalent mRNA vaccine prevents and mitigates influenza infection. *NPJ Vaccines.* 2023;8(1):157.

33. Wilson E, Goswami J, Baqui AH, Doreski PA, Perez-Marc G, Zaman K, et al. Efficacy and Safety of an mRNA-Based RSV PreF Vaccine in Older Adults. *N Engl J Med.* 2023;389(24):2233-44.

34. Kuzmin IV, Soto Acosta R, Pruitt L, Wasdin PT, Kedarinath K, Hernandez KR, et al. Comparison of uridine and N1-methylpseudouridine mRNA platforms in development of an Andes virus vaccine. *Nat Commun.* 2024;15(1):6421.

35. Ronk AJ, Lloyd NM, Zhang M, Atyeo C, Perrett HR, Mire CE, et al. A Lassa virus mRNA vaccine confers protection but does not require neutralizing antibody in a guinea pig model of infection. *Nat Commun.* 2023;14(1):5603.

36. Meyer M, Huang E, Yuzhakov O, Ramanathan P, Ciaramella G, and Bukreyev A. Modified mRNA-Based Vaccines Elicit Robust Immune Responses and Protect Guinea Pigs From Ebola Virus Disease. *J Infect Dis.* 2018;217(3):451-5.

37. Zhang P, Falcone S, Tsybovsky Y, Singh M, Gopan V, Miao H, et al. Increased neutralization potency and breadth elicited by a SARS-CoV-2 mRNA vaccine forming virus-like particles. *Proc Natl Acad Sci U S A.* 2023;120(29):e2305896120.

38. Ilinykh PA, Huang K, Santos RI, Gilchuk P, Gunn BM, Karim MM, et al. Non-neutralizing Antibodies from a Marburg Infection Survivor Mediate Protection by Fc-Effector Functions and by Enhancing Efficacy of Other Antibodies. *Cell Host Microbe.* 2020;27(6):976-91 e11.

39. Freyn AW, Pine M, Rosado VC, Benz M, Muramatsu H, Beattie M, et al. Antigen modifications improve nucleoside-modified mRNA-based influenza virus vaccines in mice. *Mol Ther Methods Clin Dev.* 2021;22:84-95.

40. Komori M, Nogimori T, Morey AL, Sekida T, Ishimoto K, Hassett MR, et al. saRNA vaccine expressing membrane-anchored RBD elicits broad and durable immunity against SARS-CoV-2

variants of concern. *Nat Commun.* 2023;14(1):2810.

41. Kolesnikova L, Berghofer B, Bamberg S, and Becker S. Multivesicular bodies as a platform for formation of the Marburg virus envelope. *J Virol.* 2004;78(22):12277-87.

42. Mittler E, Kolesnikova L, Strecker T, Garten W, and Becker S. Role of the transmembrane domain of marburg virus surface protein GP in assembly of the viral envelope. *J Virol.* 2007;81(8):3942-8.

43. Kolesnikova L, Mittler E, Schudt G, Shams-Eldin H, and Becker S. Phosphorylation of Marburg virus matrix protein VP40 triggers assembly of nucleocapsids with the viral envelope at the plasma membrane. *Cell Microbiol.* 2012;14(2):182-97.

44. Mathieu NA, Paparisto E, Barr SD, and Spratt DE. HERC5 and the ISGylation Pathway: Critical Modulators of the Antiviral Immune Response. *Viruses.* 2021;13(6).

45. Xia C, Bao Z, Tabassam F, Ma W, Qiu M, Hua S, et al. GCIP, a novel human grap2 and cyclin D interacting protein, regulates E2F-mediated transcriptional activity. *J Biol Chem.* 2000;275(27):20942-8.

46. Vladimer GI, Gorna MW, and Superti-Furga G. IFITs: Emerging Roles as Key Anti-Viral Proteins. *Front Immunol.* 2014;5:94.

47. Woolsey C, Borisevich V, Agans KN, Fenton KA, Cross RW, and Geisbert TW. Bundibugyo ebolavirus Survival Is Associated with Early Activation of Adaptive Immunity and Reduced Myeloid-Derived Suppressor Cell Signaling. *mBio.* 2021;12(4):e0151721.

48. Biji A, Khatun O, Swaraj S, Narayan R, Rajmani RS, Sardar R, et al. Identification of COVID-19 prognostic markers and therapeutic targets through meta-analysis and validation of Omics data from nasopharyngeal samples. *EBioMedicine.* 2021;70:103525.

49. Mire CE, Geisbert JB, Agans KN, Satterfield BA, Versteeg KM, Fritz EA, et al. Durability of a vesicular stomatitis virus-based marburg virus vaccine in nonhuman primates. *PLoS One.* 2014;9(4):e94355.

50. Keshwara R, Hagen KR, Abreu-Mota T, Papaneri AB, Liu D, Wirblich C, et al. A Recombinant Rabies Virus Expressing the Marburg Virus Glycoprotein Is Dependent upon Antibody-Mediated

717 Cellular Cytotoxicity for Protection against Marburg Virus Disease in a Murine Model. *J Virol.*
718 2019;93(6): 01865-18.
719 51. Ilinykh PA, Santos RI, Gunn BM, Kuzmina NA, Shen X, Huang K, et al. Asymmetric antiviral effects
720 of ebolavirus antibodies targeting glycoprotein stem and glycan cap. *PLoS Pathog.*
721 2018;14(8):e1007204.
722 52. O'Donnell KL, Feldmann F, Kaza B, Clancy CS, Hanley PW, Fletcher P, et al. Rapid protection of
723 nonhuman primates against Marburg virus disease using a single low-dose VSV-based vaccine.
724 *EBioMedicine.* 2023;89:104463.
725 53. Geisbert TW, Bailey M, Geisbert JB, Asiedu C, Roederer M, Grazia-Pau M, et al. Vector choice
726 determines immunogenicity and potency of genetic vaccines against Angola Marburg virus in
727 nonhuman primates. *J Virol.* 2010;84(19):10386-94.
728 54. Stonier SW, Herbert AS, Kuehne AI, Sobarzo A, Habibulin P, Dahan CVA, et al. Marburg virus
729 survivor immune responses are Th1 skewed with limited neutralizing antibody responses. *J Exp*
730 *Med.* 2017;214(9):2563-72.
731 55. Fabozzi G, Nabel CS, Dolan MA, and Sullivan NJ. Ebolavirus proteins suppress the effects of
732 small interfering RNA by direct interaction with the mammalian RNA interference pathway. *J Virol.*
733 2011;85(6):2512-23.
734 56. Valmas C, Grosch MN, Schumann M, Olejnik J, Martinez O, Best SM, et al. Marburg virus evades
735 interferon responses by a mechanism distinct from ebola virus. *PLoS Pathog.*
736 2010;6(1):e1000721.
737 57. Valmas C, and Basler CF. Marburg virus VP40 antagonizes interferon signaling in a species-
738 specific manner. *J Virol.* 2011;85(9):4309-17.
739 58. Prator CA, Dorratt BM, O'Donnell KL, Lack J, Pinski AN, Ricklefs S, et al. Transcriptional profiling
740 of immune responses in NHPs after low-dose, VSV-based vaccination against Marburg virus.
741 *Emerg Microbes Infect.* 2023;12(2):2252513.
742 59. Connor JH, Yen J, Caballero IS, Garamszegi S, Malhotra S, Lin K, et al. Transcriptional Profiling
743 of the Immune Response to Marburg Virus Infection. *J Virol.* 2015;89(19):9865-74.

60. Olejnik J, Hume AJ, Leung DW, Amarasinghe GK, Basler CF, and Muhlberger E. Filovirus Strategies to Escape Antiviral Responses. *Curr Top Microbiol Immunol.* 2017;411:293-322.

61. Warfield KL, Howell KA, Vu H, Geisbert J, Wong G, Shulenin S, et al. Role of Antibodies in Protection Against Ebola Virus in Nonhuman Primates Immunized With Three Vaccine Platforms. *J Infect Dis.* 2018;218(suppl_5):S553-S64.

62. Hevey M, Negley D, Pushko P, Smith J, and Schmaljohn A. Marburg virus vaccines based upon alphavirus replicons protect guinea pigs and nonhuman primates. *Virology.* 1998;251(1):28-37.

63. Zhang P, Singh M, Becker VA, Croft J, Tsybovsky Y, Gopan V, et al. Inclusion of a retroviral protease enhances the immunogenicity of VLP-forming mRNA vaccines against HIV-1 or SARS-CoV-2 in mice. *Sci Transl Med.* 2025;17(796):eadt9576.

64. Melzi E, Willis JR, Ma KM, Lin YC, Kratochvil S, Berndsen ZT, et al. Membrane-bound mRNA immunogens lower the threshold to activate HIV Env V2 apex-directed broadly neutralizing B cell precursors in humanized mice. *Immunity.* 2022;55(11):2168-86 e6.

65. Towner JS, Khristova ML, Sealy TK, Vincent MJ, Erickson BR, Bawiec DA, et al. Marburgvirus genomics and association with a large hemorrhagic fever outbreak in Angola. *J Virol.* 2006;80(13):6497-516.

66. Bolger AM, Lohse M, and Usadel B. Trimmomatic: a flexible trimmer for Illumina sequence data. *Bioinformatics.* 2014;30(15):2114-20.

67. Dobin A, Davis CA, Schlesinger F, Drenkow J, Zaleski C, Jha S, et al. STAR: ultrafast universal RNA-seq aligner. *Bioinformatics.* 2013;29(1):15-21.

68. Love MI, Huber W, and Anders S. Moderated estimation of fold change and dispersion for RNA-seq data with DESeq2. *Genome Biol.* 2014;15(12):550.

69. Szklarczyk D, Franceschini A, Wyder S, Forslund K, Heller D, Huerta-Cepas J, et al. STRING v10: protein-protein interaction networks, integrated over the tree of life. *Nucleic Acids Res.* 2015;43(Database issue):D447-52.

70. Heberle H, Meirelles GV, da Silva FR, Telles GP, and Minghim R. InteractiVenn: a web-based tool for the analysis of sets through Venn diagrams. *BMC Bioinformatics.* 2015;16(1):169.

FIGURE LEGENDS

Figure 1. Optimization of MARV VLPs generation from GP and VP40 mRNA in HEK293T cells.

(**A**) Schematic of MARV GP and VLP mRNA-LNP vaccines.

(**B**) Immunoblots of GP and VP40 mRNA transfected HEK293T cell lysates.

(**C**) Immunoblots of GP and VP40 for the sucrose cushion concentrated VLPs.

(**D** and **E**) The indicated concentrations of GP mRNA (μg) were transfected with VP40 mRNA in HEK293T cells to determine the optimal ratio for VLP generation: Immunoblots of cell lysates (**D**) and VLPs (**E**); GAPDH loading control.

(**F** and **G**) A comparison of the intensity of GP and VP40 bands in D and E blots. Molecular weights in kDa are shown at the left.

Figure 2. Electron microscopy of MARV VLPs.

(**A**) HEK293T cells transfected with GP mRNA (control). The arrow indicates a membrane protrusion.

(**B**) VLPs in HEK293T cells transfected with GP and VP40 mRNA. The arrow indicates VLP structures.

(**C**) Negative staining of VLPs.

(**D**) Immunogold and negative staining of VLPs. The arrow indicates gold nanoparticle deposition.

Figure 3. A comparison of surface staining of membrane-bound GP protein levels in mRNA transfected cells.

(**A**) Representative flow cytometry plots for 24 h incubation.

(**B**) Percentages of GP^+ HEK293T cells.

(**C**) Median fluorescence intensity (MFI) of GP^+ HEK293T cells.

(**D**) Percentages of GP^+ Vero E6 cells.

(**E**) MFI of GP+ Vero E6 cells.

Data are represented as a mean ± SEM. Statistical significance was calculated by one-way ANOVA analysis followed by Tukey's multiple comparison test.

Figure 4. Assessment of MARV GP and VLP mRNA vaccine in guinea pig Study 1: immunogenicity.

(**A**) Study design: Guinea pigs (*n=5*) were vaccinated with GP mRNA (green) or VLP mRNA (red) via the intramuscular route on days 0 and 29. Serum samples were collected on days 27 and 54. On day 56, guinea pigs were challenged with guinea pig-adapted MARV, and serum samples were collected on the indicated days for viremia analysis. The study was terminated on day 28 post-challenge.

(**B**) MARV GP-specific ELISA absorbance values.

(**C**) GP IgG antibody titers.

(**D**) MARV VP40-specific-binding ELISA absorbance values.

(**E**) VP40 IgG antibody titers.

(**F**) MARV neutralizing antibody responses expressed as a percentage reduction of plaque count.

(**G**) $PRNT_{60}$ titer.

Data are represented as medians and interquartile ranges (**B–G**). Statistical significance was calculated by Kruskal–Wallis analysis followed by Dunn's multiple comparison test (**C, E, G**).

Figure 5. Assessment of MARV GP and VLP mRNA vaccine in guinea pig study 1: protective efficacy.

(**A**) Survival curve.

(**B**) Percent body weight change.

(**C**) Disease score.

(**D**) Viremia.

(**E, F, G**) Viral load in the spleen, liver, and kidneys, respectively.

Data are represented as individual values (**A, C, D**) and median and interquartile ranges (**B, E, F, G**). The Log Rank (Mantel-Cox) test was used to analyze the survival data. Statistical significance was calculated

by two-way ANOVA analysis followed by Dunnett's multiple comparison test (**B**) and Kruskal–Wallis test followed by Dunn's multiple comparison test (**E, F, G**). # Same p-value for all vaccinated groups vs. NTFIX (control).

Figure 6. Assessment of MARV GP and VLP mRNA vaccine in guinea pig study 2: immunogenicity.

(**A**) Study design: Guinea pigs (*n=5*) were vaccinated with GP mRNA (green) or VLP mRNA (red). The study was conducted as described in Study 1.

(**B** and **C**) MARV GP-specific ELISA absorbance values.

(**D**) GP IgG antibody titers.

(**E** and **F**) MARV VP40-specific-binding ELISA absorbance values.

(**G**) VP40 IgG antibody titers.

(H and **I**) MARV neutralizing antibody responses expressed as a percentage reduction of plaque count.

(**J**) $PRNT_{60}$ titer.

Data are represented as medians and interquartile ranges (**B–J**). Statistical significance was calculated by Kruskal–Wallis analysis followed by Dunn's multiple comparison test (**D, G, J**).

Figure 7. Assessment of MARV GP and VLP mRNA vaccine in guinea pig study 2: protective efficacy.

(**A**) Survival curve.

(B and **C)** Percent body weight change.

(**D**) Disease score.

(**E**) Viremia.

(**F-H**) Viral load in the spleen, liver, and kidneys, respectively.

Data are represented as individual values (**A-D, E**) and median and interquartile ranges (**F, G, H**). The Log Rank (Mantel-Cox) test was used to analyze the survival data. Statistical significance was calculated by two-way ANOVA analysis followed by Dunnett's multiple comparison test (**B**) and Kruskal–Wallis test

850 followed by Dunn's multiple comparison test (**F, G, H**). # Same p-value for all vaccinated groups vs. PBS
851 (control); otherwise, values were indicated.
852
853 **Figure 8. Histopathology of liver and spleen tissues of control and vaccinated groups from the**
854 **dose-down study.** Liver and spleen tissues collected from the guinea pigs were stained with hematoxylin
855 and eosin. # For the VLP group (1.33 μg and 4 μg), the images represent the guinea pigs that succumbed
856 to infection. Scale bar = 100 μM.
857 (**A**) The control liver section shows the following characteristics: Apoptosis/necrosis (red asterisk),
858 hepatocellular vacuolation (red arrow), and councilman-like bodies (black arrow).
859 (**B–D**) Liver sections from the indicated vaccine group.
860 (**E**) The control spleen section shows apoptosis/necrosis in the red pulp (red asterisk) and lymphocyte
861 depletion in the white pulp (blue arrow).
862 (**F-H**) Spleen sections from the indicated vaccine group.
863
864 **Figure 9. MARV GP-specific T-cell responses to GP and VLP mRNA vaccines.**
865 (**A**) Study design: Six to seven-week-old female BALB/c mice (*n*=*5*) were vaccinated with GP mRNA
866 (green) or VLP mRNA (red) via the intramuscular route on days 0 and 29. Control mice received PBS
867 (black). Spleens were collected and processed to isolate splenocytes. Splenocytes were stimulated with
868 DMSO or GP-peptide pool to measure GP-specific $CD4^+$ and $CD8^+$ T cells by flow cytometry.
869 (**B**) Percentages of the indicated cell populations.
870 (**C**)Percentages of total $CD4^+$ T cells producing the indicated cytokines. Each bar indicates the individual
871 % $CD4^+$ T cells value of each mouse.
872 (**D**) Percentages of total $CD8^+$ T cells producing the indicated cytokines. Each bar indicates the individual
873 % $CD8^+$ T cells value of each mouse.
874 Data are represented as medians and interquartile ranges (B–G) and values for individual animals (C,
875 D). Statistical significance was calculated by Kruskal–Wallis analysis followed by Dunn's multiple
876 comparison test (B to G).

Figure 10. GP mRNA vaccine induces minimal changes in the guinea pig whole blood transcriptome as compared to the VLP mRNA vaccine.

A. Principal component analysis (PCA) of genes expressed in control and vaccinated groups**.**

B. A total number of up and down regulated genes in the whole blood of vaccinated groups versus PBS. The graph shows genes with log2 (fold change) ≥1 and adjusted p-vales of ≤ 0.05.

C. Functional enrichment analysis of significantly differentially expressed genes.

D. Venn diagram of overlapping genes between *GP* and *VLP* mRNA vaccinated groups versus PBS.

E. List of overlapping genes between GP and VLP mRNA vaccinated groups versus PBS with log2 (fold change) values. Arrowheads pointing up or down indicate up and downregulated genes, respectively.

Figure 11. Vaccinated guinea pig groups show reduced expression of antiviral response genes compared to the unvaccinated group.

A. Principal component analysis (PCA) of genes expressed in control and vaccinated groups. The two outlier samples from the control group were removed for better visualization.

B. Total numbers of up and downregulated genes in the whole blood of vaccinated groups versus PBS. The graph shows genes with log2(fold change) ≥1 and adjusted p-vales of ≤ 0.05.

C. Venn diagram showing the intersection of overlapping downregulated genes among all vaccinated groups versus PBS.

D. Functional enrichment analysis of overlapping downregulated genes.

E. Genes related to immune response and apoptosis with log2(fold change) values.

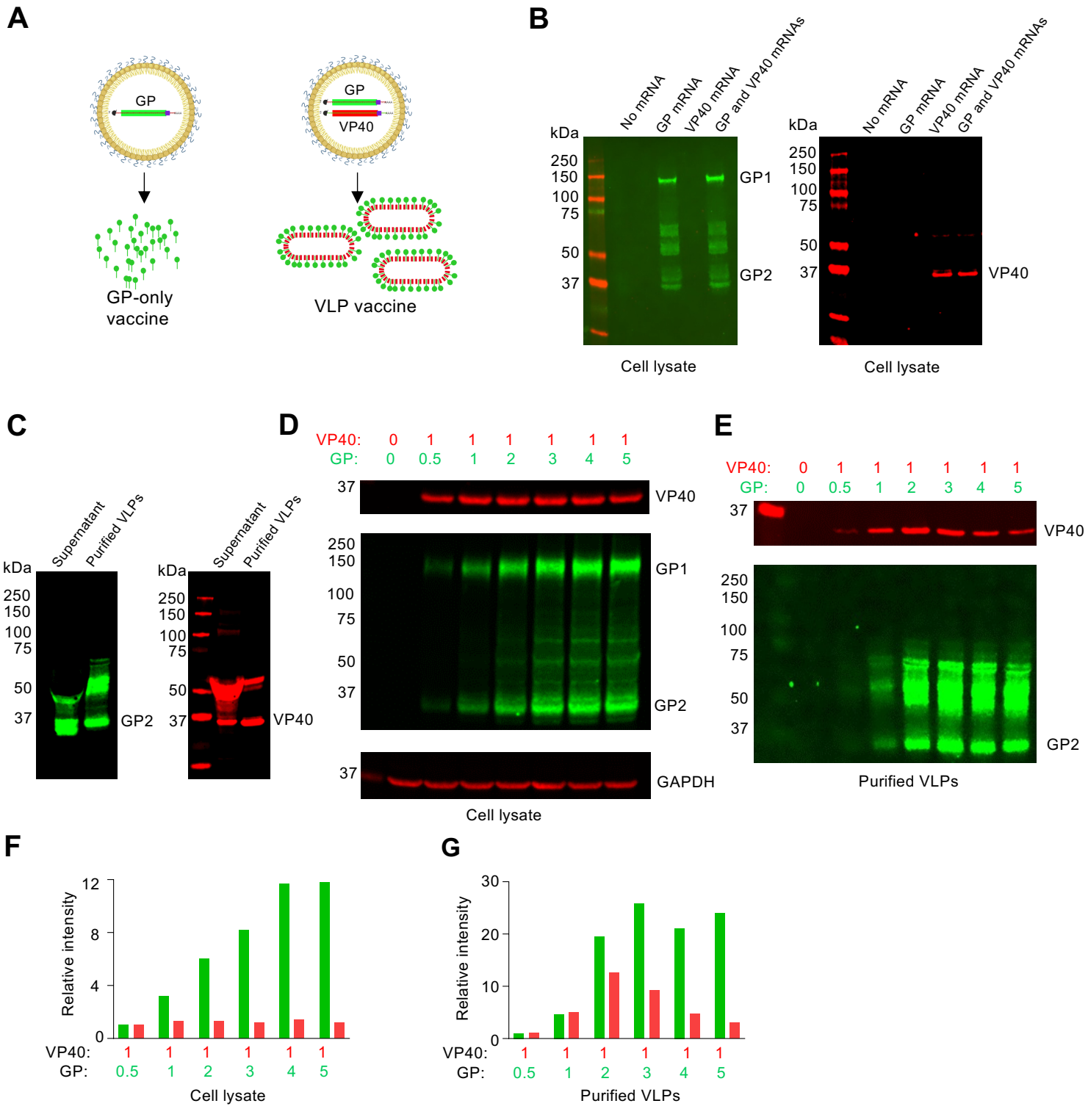

Figure 1. Optimization of MARV VLPs generation from GP and VP40 mRNA in HEK293T cells.

(**A**) Schematic of MARV GP and VLP mRNA-LNP vaccines.

(**B**) Immunoblots of GP and VP40 mRNA transfected HEK293T cell lysates.

(**C**) Immunoblots of GP and VP40 for the sucrose cushion concentrated VLPs.

(**D** and **E**) The indicated concentrations of GP mRNA (μg) were transfected with VP40 mRNA in HEK293T cells to determine the optimal ratio for VLP generation: Immunoblots of cell lysates (**D**) and VLPs (**E**); GAPDH loading control.

(**F** and **G**) A comparison of the intensity of GP and VP40 bands in D and E blots. Molecular weights in kDa are shown at the left.

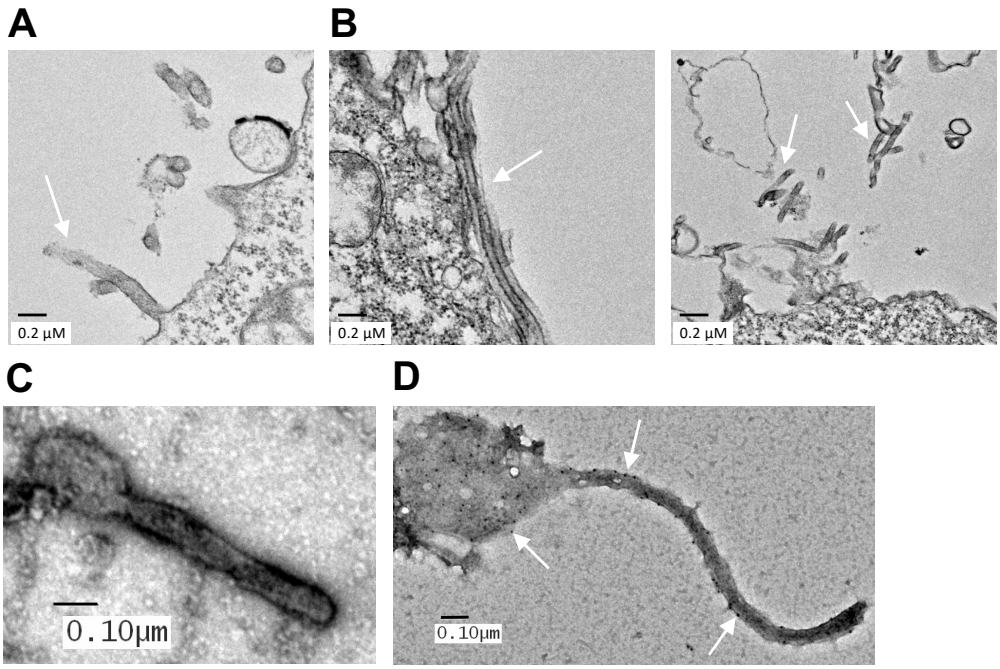

Figure 2. Electron microscopy of MARV VLPs.

(**A**) HEK293T cells transfected with GP mRNA (control). The arrow indicates a membrane protrusion.

(**B**) VLPs in HEK293T cells transfected with GP and VP40 mRNA. The arrow indicates VLP structures.

(**C**) Negative staining of VLPs.

(**D**) Immunogold and negative staining of VLPs. The arrow indicates gold nanoparticle deposition.

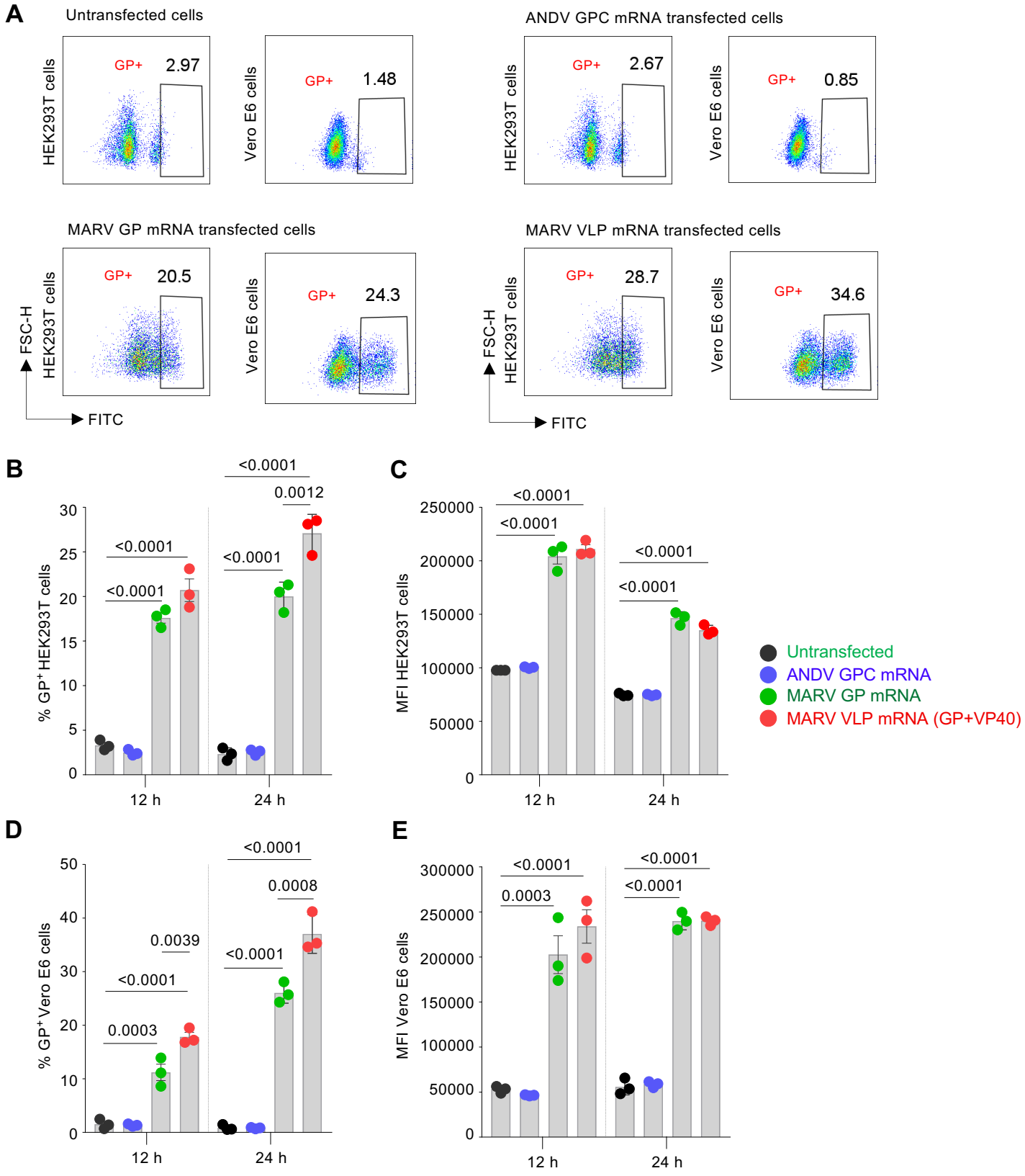

Figure 3. A comparison of surface staining of membrane-bound GP protein levels in mRNA transfected cells.
(**A**) Representative flow cytometry plots for 24 h incubation.
(**B**) Percentages of GP⁺ HEK293T cells.
(**C**) Median fluorescence intensity (MFI) of GP⁺ HEK293T cells.
(**D**) Percentages of GP⁺ Vero E6 cells.
(**E**) MFI of GP+ Vero E6 cells.
Data are represented as a mean ± SEM. Statistical significance was calculated by one-way ANOVA analysis followed by Tukey's multiple comparison test.

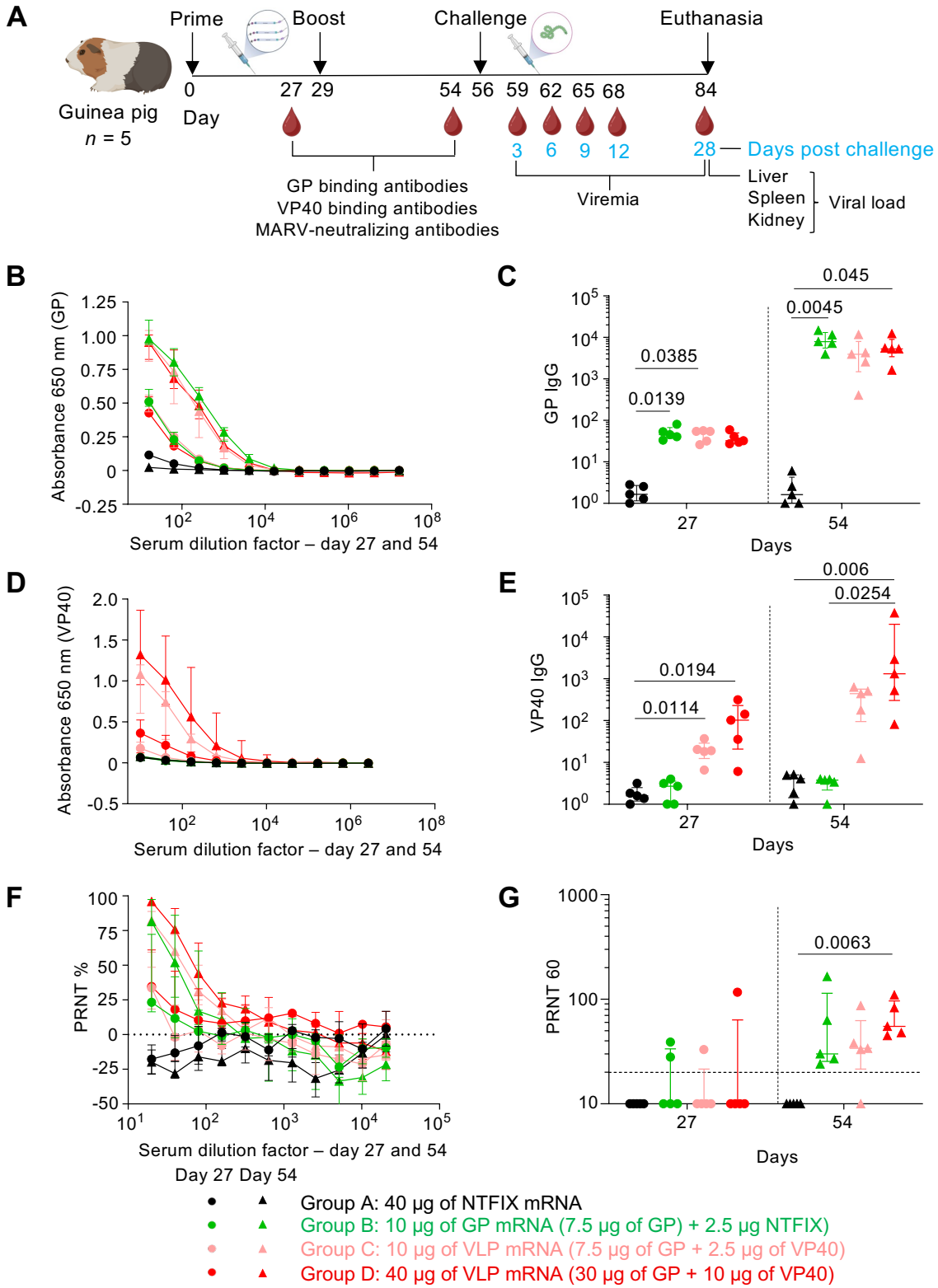

Figure 4. Assessment of MARV GP and VLP mRNA vaccine in guinea pig Study 1: immunogenicity.

(**A**) Study design: Guinea pigs (*n=5*) were vaccinated with GP mRNA (green) or VLP mRNA (red) via the intramuscular route on days 0 and 29. Serum samples were collected on days 27 and 54. On day 56, guinea pigs were challenged with guinea pig-adapted MARV, and serum samples were collected on the indicated days for viremia analysis. The study was terminated on day 28 post-challenge.

(**B**) MARV GP-specific ELISA absorbance values.

(**C**) GP IgG antibody titers.

(**D**) MARV VP40-specific-binding ELISA absorbance values.

(**E**) VP40 IgG antibody titers.

(**F**) MARV neutralizing antibody responses expressed as a percentage reduction of plaque count.

(**G**) $PRNT_{60}$ titer.

Data are represented as medians and interquartile ranges (**B–G**). Statistical significance was calculated by Kruskal–Wallis analysis followed by Dunn's multiple comparison test (**C, E, G**).

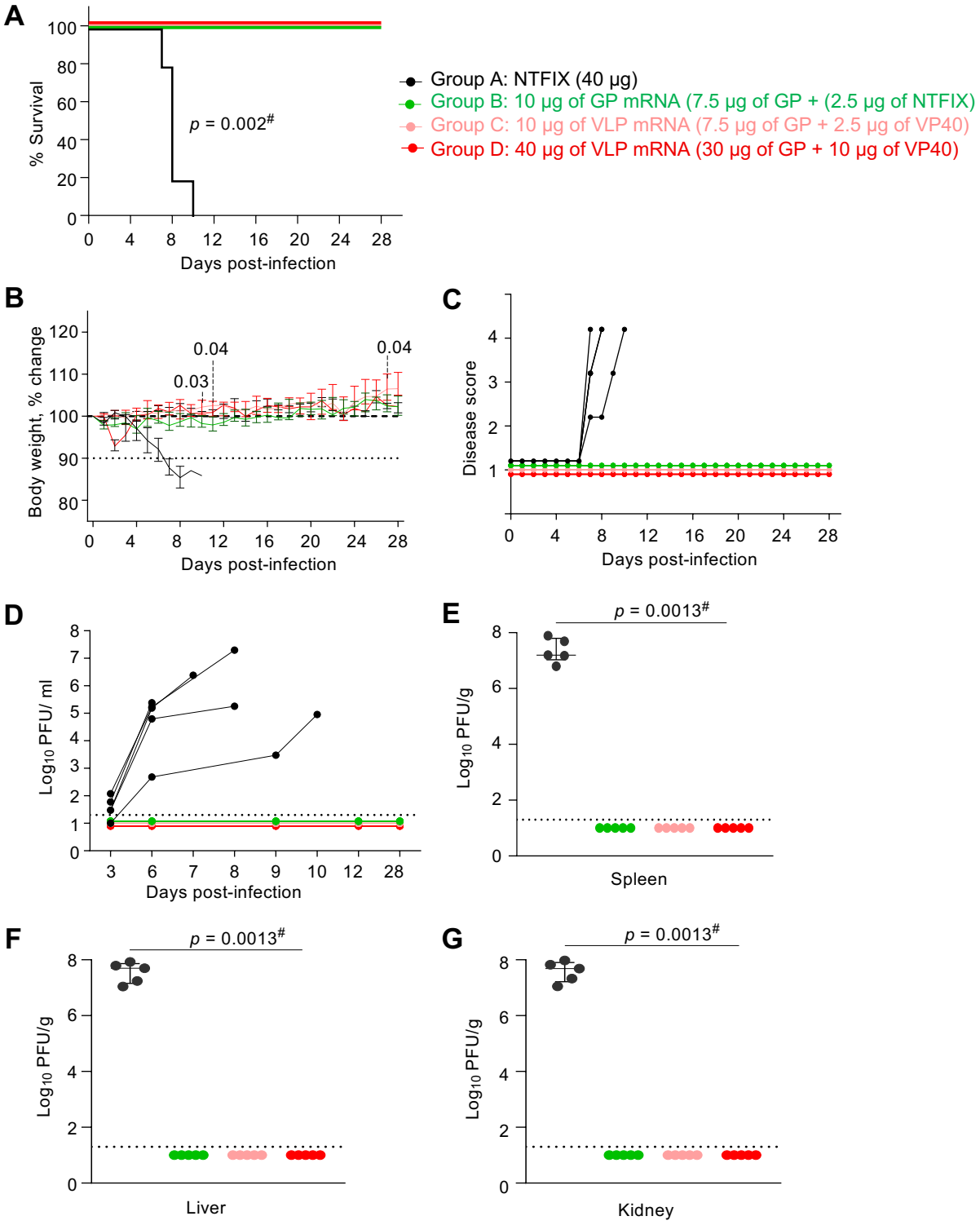

Figure 5. Assessment of MARV GP and VLP mRNA vaccine in guinea pig Study 1: protective efficacy.
(**A**) Survival curve.
(**B**) Percent body weight change.
(**C**) Disease score.
(**D**) Viremia.
(**E, F, G**) Viral load in the spleen, liver, and kidneys, respectively.
Data are represented as individual values (**A, C, D**) and median and interquartile ranges (**B, E, F, G**). The Log Rank (Mantel-Cox) test was used to analyze the survival data. Statistical significance was calculated by two-way ANOVA analysis followed by Dunnett's multiple comparison test (**B**) and Kruskal–Wallis test followed by Dunn's multiple comparison test (**E, F, G**). # Same p-value for all vaccinated groups vs. NTFIX (control).

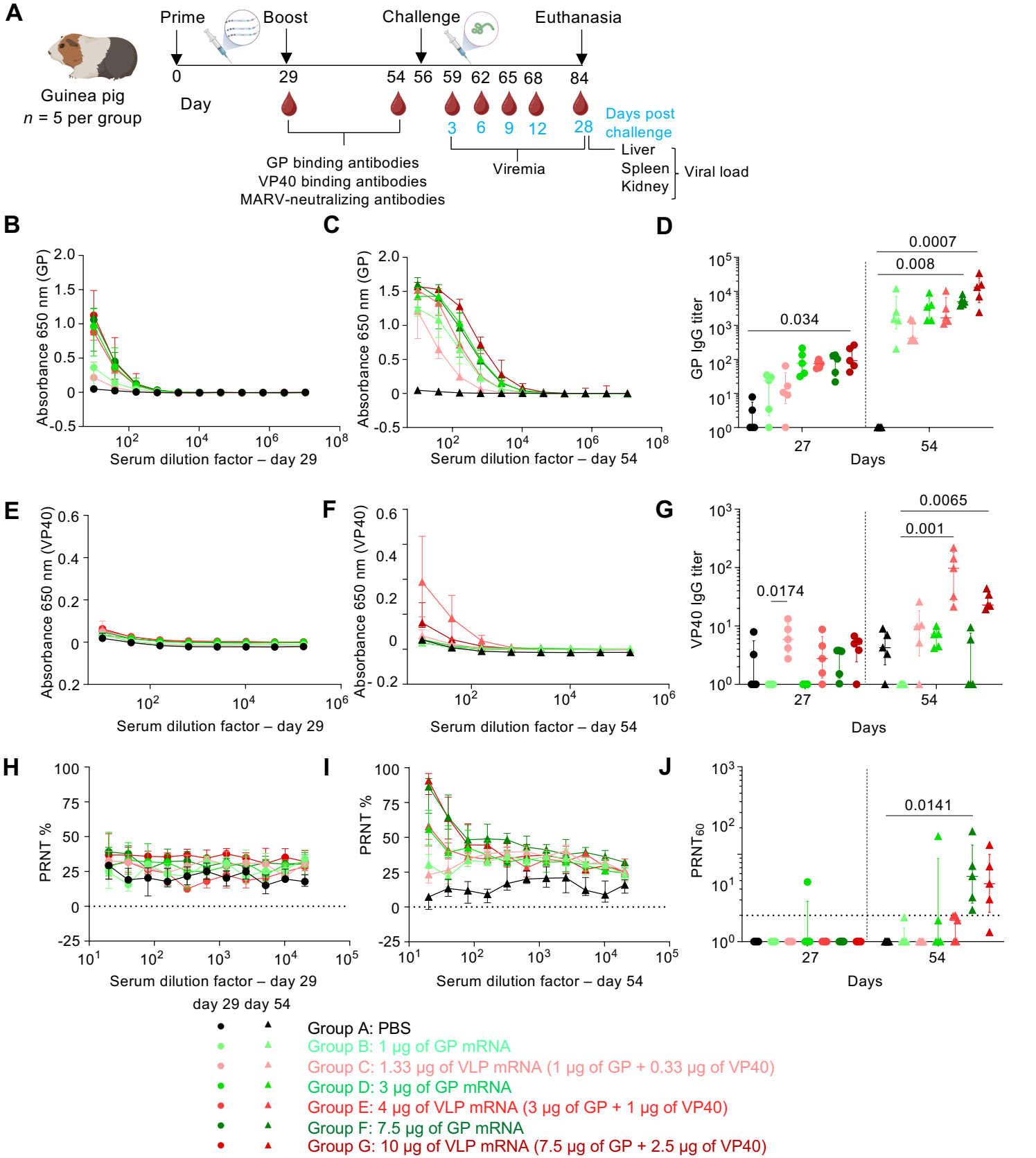
A
Guinea pig
n = 5 per group
Prime
Boost
Challenge
Euthanasia
0
29
54
56
59
62
65
68
84
Day
3
6
9
12
28
Days post challenge
GP binding antibodies
VP40 binding antibodies
MARV-neutralizing antibodies
Viremia
Liver
Spleen
Kidney
Viral load
B
Absorbance 650 nm (GP)
Serum dilution factor – day 29
C
Absorbance 650 nm (GP)
Serum dilution factor – day 54
D
GP IgG titer
0.034
0.0007
0.008
27
54
Days
E
Absorbance 650 nm (VP40)
Serum dilution factor – day 29
F
Absorbance 650 nm (VP40)
Serum dilution factor – day 54
G
VP40 IgG titer
0.0174
0.0065
0.001
27
54
Days
H
PRNT %
Serum dilution factor – day 29
day 29 day 54
I
PRNT %
Serum dilution factor – day 54
J
PRNT60
0.0141
27
54
Days
Group A: PBS
Group B: 1 µg of GP mRNA
Group C: 1.33 µg of VLP mRNA (1 µg of GP + 0.33 µg of VP40)
Group D: 3 µg of GP mRNA
Group E: 4 µg of VLP mRNA (3 µg of GP + 1 µg of VP40)
Group F: 7.5 µg of GP mRNA
Group G: 10 µg of VLP mRNA (7.5 µg of GP + 2.5 µg of VP40)

Figure 6. Assessment of MARV GP and VLP mRNA vaccine in guinea pig Study 2: immunogenicity.
(**A**) Study design: Guinea pigs (*n=5*) were vaccinated with GP mRNA (green) or VLP mRNA (red). The study was conducted as described in Study 1.
(**B** and **C**) MARV GP-specific ELISA absorbance values.
(**D**) GP IgG antibody titers.
(**E** and **F**) MARV VP40-specific-binding ELISA absorbance values.
(**G**) VP40 IgG antibody titers.
(H and **I**) MARV neutralizing antibody responses expressed as a percentage reduction of plaque count.
(**J**) $PRNT_{60}$ titer.
Data are represented as medians and interquartile ranges (**B–J**). Statistical significance was calculated by Kruskal–Wallis analysis followed by Dunn's multiple comparison test (**D, G, J**).

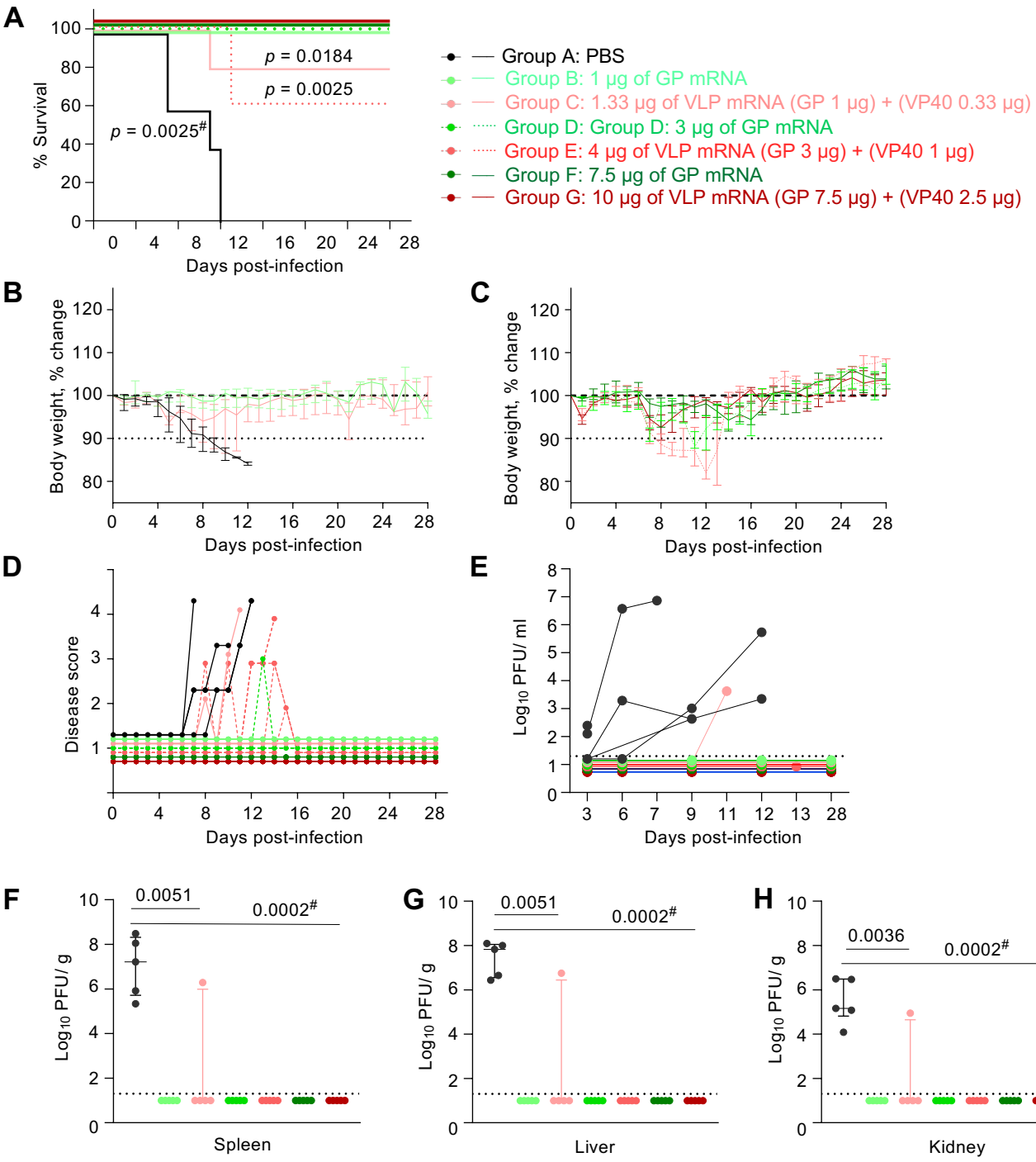

Figure 7. Assessment of MARV GP and VLP mRNA vaccine in guinea pig Study 2: protective efficacy.
(**A**) Survival curve.
(B and **C)** Percent body weight change.
(**D**) Disease score.
(**E**) Viremia.
(**F-H**) Viral load in the spleen, liver, and kidneys, respectively.
Data are represented as individual values (**A-D, E**) and median and interquartile ranges (**F, G, H**). The Log Rank (Mantel-Cox) test was used to analyze the survival data. Statistical significance was calculated by two-way ANOVA analysis followed by Dunnett's multiple comparison test (**B**) and Kruskal–Wallis test followed by Dunn's multiple comparison test (**F, G, H**). # Same p-value for all vaccinated groups vs. PBS (control); otherwise, values were indicated.

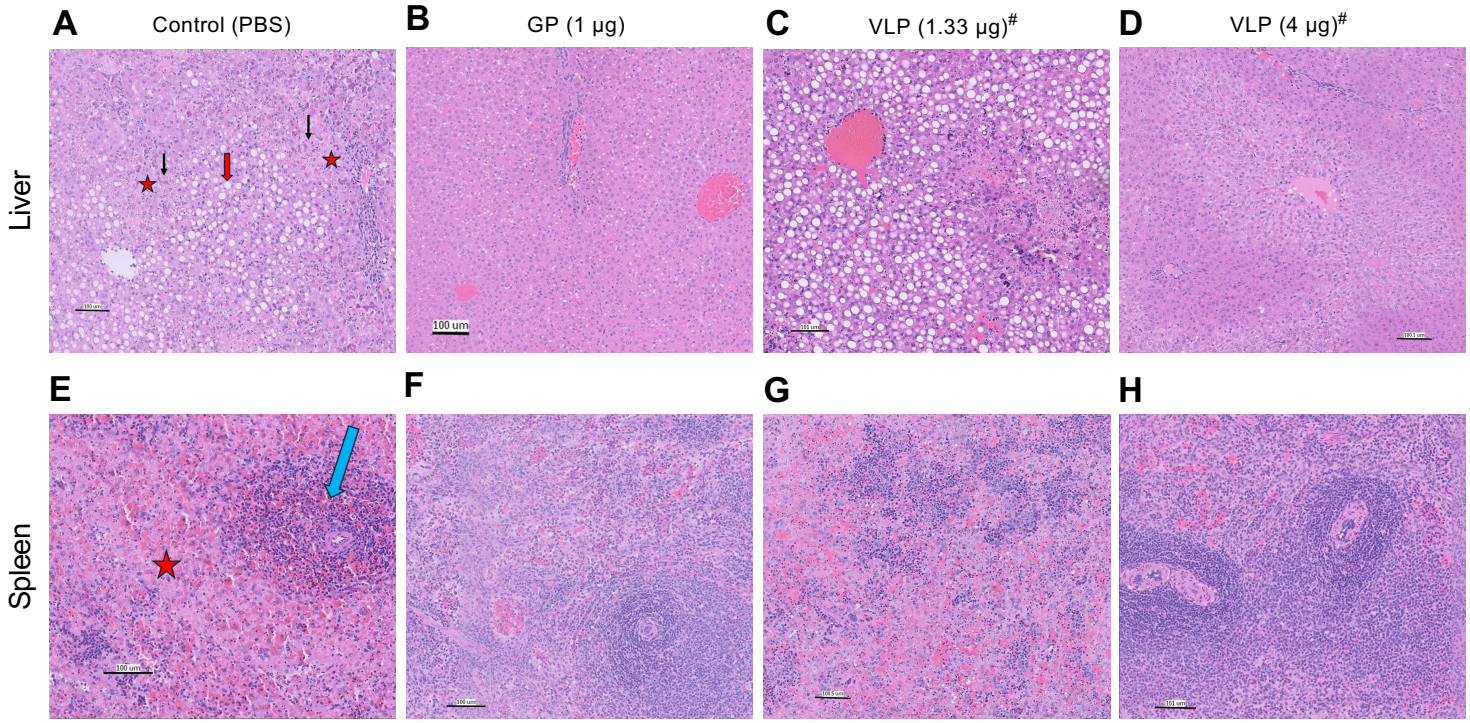

Figure 8. Histopathology of liver and spleen tissues of control and vaccinated groups from the guinea pig Study 2.
Liver and spleen tissues collected from the guinea pigs were stained with hematoxylin and eosin. # For the VLP group (1.33 µg and 4 µg), the images represent the guinea pigs that succumbed to infection. Scale bar = 100 µM.
(**A**) The control liver section shows the following characteristics: Apoptosis/necrosis (red asterisk), hepatocellular vacuolation (red arrow), and councilman-like bodies (black arrow).
(**B–D**) Liver sections from the indicated vaccine group.
(**E**) The control spleen section shows apoptosis/necrosis in the red pulp (red asterisk) and lymphocyte depletion in the white pulp (blue arrow).
(**F-H**) Spleen sections from the indicated vaccine group.

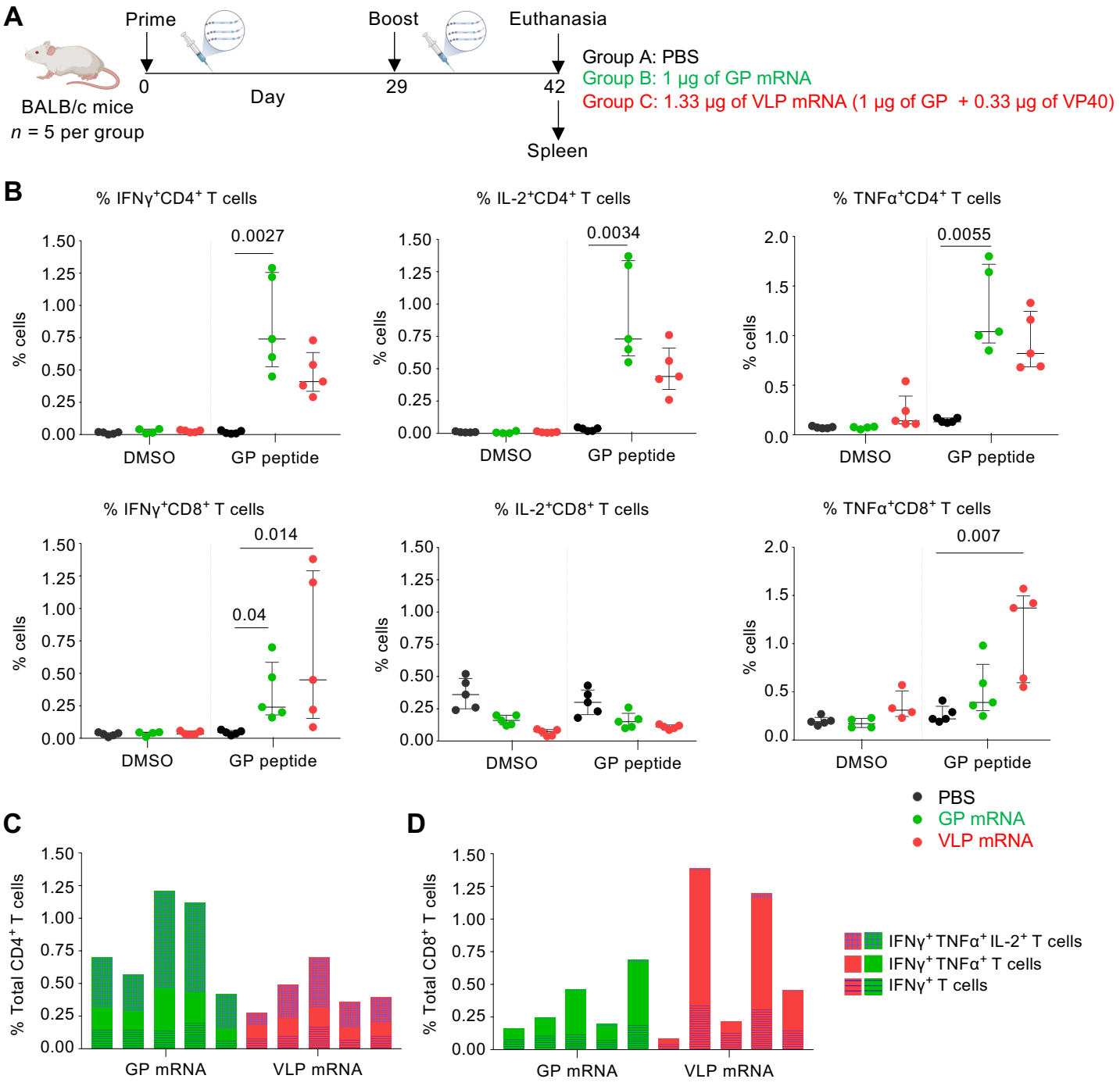

Figure 9. MARV GP-specific T-cell responses to GP and VLP mRNA vaccines.
(**A**) Study design: Six to seven-week-old female BALB/c mice (*n=5*) were vaccinated with GP mRNA (green) or VLP mRNA (red) via the intramuscular route on days 0 and 29. Control mice received PBS (black). Spleens were collected and processed to isolate splenocytes. Splenocytes were stimulated with DMSO or GP-peptide pool to measure GP-specific $CD4^+$ and $CD8^+$ T cells by flow cytometry.
(**B**) Percentages of the indicated cell populations.
(**C**)Percentages of total $CD4^+$ T cells producing the indicated cytokines. Each bar indicates the individual % $CD4^+$ T cells value of each mouse.
(**D**) Percentages of total $CD8^+$ T cells producing the indicated cytokines. Each bar indicates the individual % $CD8^+$ T cells value of each mouse.
Data are represented as medians and interquartile ranges (B–G) and values for individual animals (C, D). Statistical significance was calculated by Kruskal–Wallis analysis followed by Dunn's multiple comparison test (B to G).

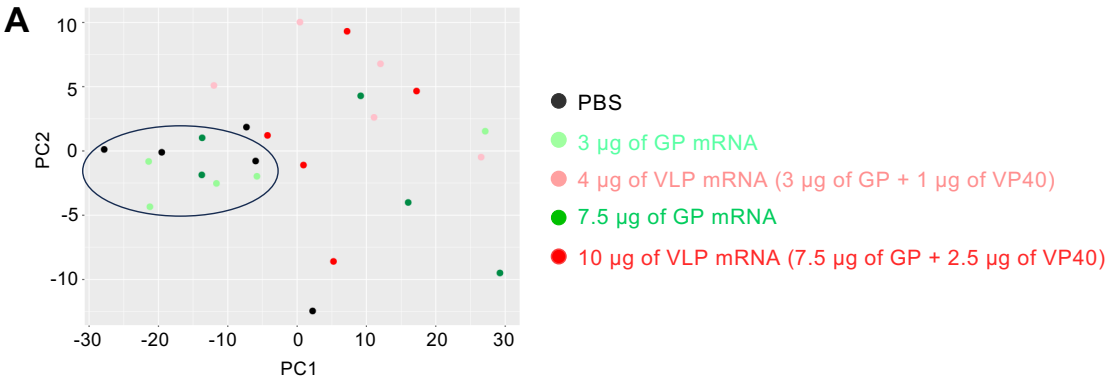

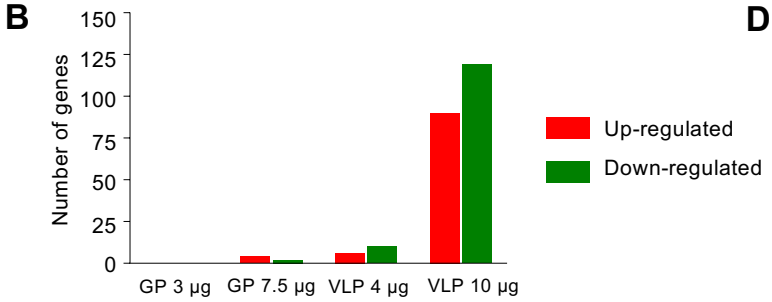

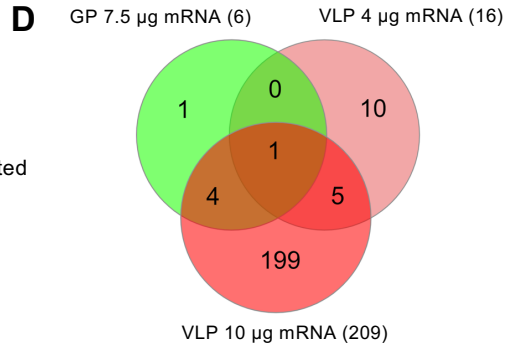

C

GP 7.5 vs PBS ↑	Reactome: Interferon signaling Reactome: ISG15 antiviral mechanism Reactome: Antiviral mechanism by IFN-stimulated genes
VLP 10 vs PBS ↑	Compartments: Mitochondrial respirasome Compartments: Respiratory chain complex
VLP 10 vs PBS ↓	GO Process: Positive regulation of biological process GO Process: Positive regulation of cellular process GO Process: Positive regulation of metabolic process GO Process: Regulation of cellular metabolic process GO Process: Negative regulation of cellular metabolic process KEGG: NF-kappa B signaling pathway Reactome: Post-transcriptional silencing by small RNAs
VLP 10 vs VLP 4 ↓	KEGG: Natural killer cell mediated cytotoxicity KEGG: B cell receptor signaling pathway KEGG: Fc gamma R-mediated phagocytosis KEGG: NF-kappa B signaling pathway

E

	GP 7.5 µg	VLP 10 µg	VLP 4 µg
SIK1	-1.17	-2.03	-1.08
HERC5	1.78	1.16	
CCNDBP1	1.57	1.28	
IFIT1B	1.25	1.09	
RGS1	-1.07	-1.06	
HMNC2		24.82	22.94
LOC100735514		1.34	1.84
PDLIM4		1.05	1.26
NR4A2		-1.96	-1.27
LOC100735368		-1.28	-1.59

Figure 10. GP mRNA vaccine induces minimal changes in the guinea pigs whole blood transcriptome as compared to the VLP mRNA vaccine.

A. Principal component analysis (PCA) of genes expressed in control and vaccinated groups**.**

B. A total number of up and down regulated genes in the whole blood of vaccinated groups versus PBS. The graph shows genes with log2 (fold change) ≥1 and adjusted p-vales of ≤ 0.05.

C. Functional enrichment analysis of significantly differentially expressed genes.

D. Venn diagram of overlapping genes between *GP* and *VLP* mRNA vaccinated groups versus PBS.

E. List of overlapping genes between GP and VLP mRNA vaccinated groups versus PBS with log2 (fold change) values. Arrowheads pointing up or down indicate up and downregulated genes, respectively.

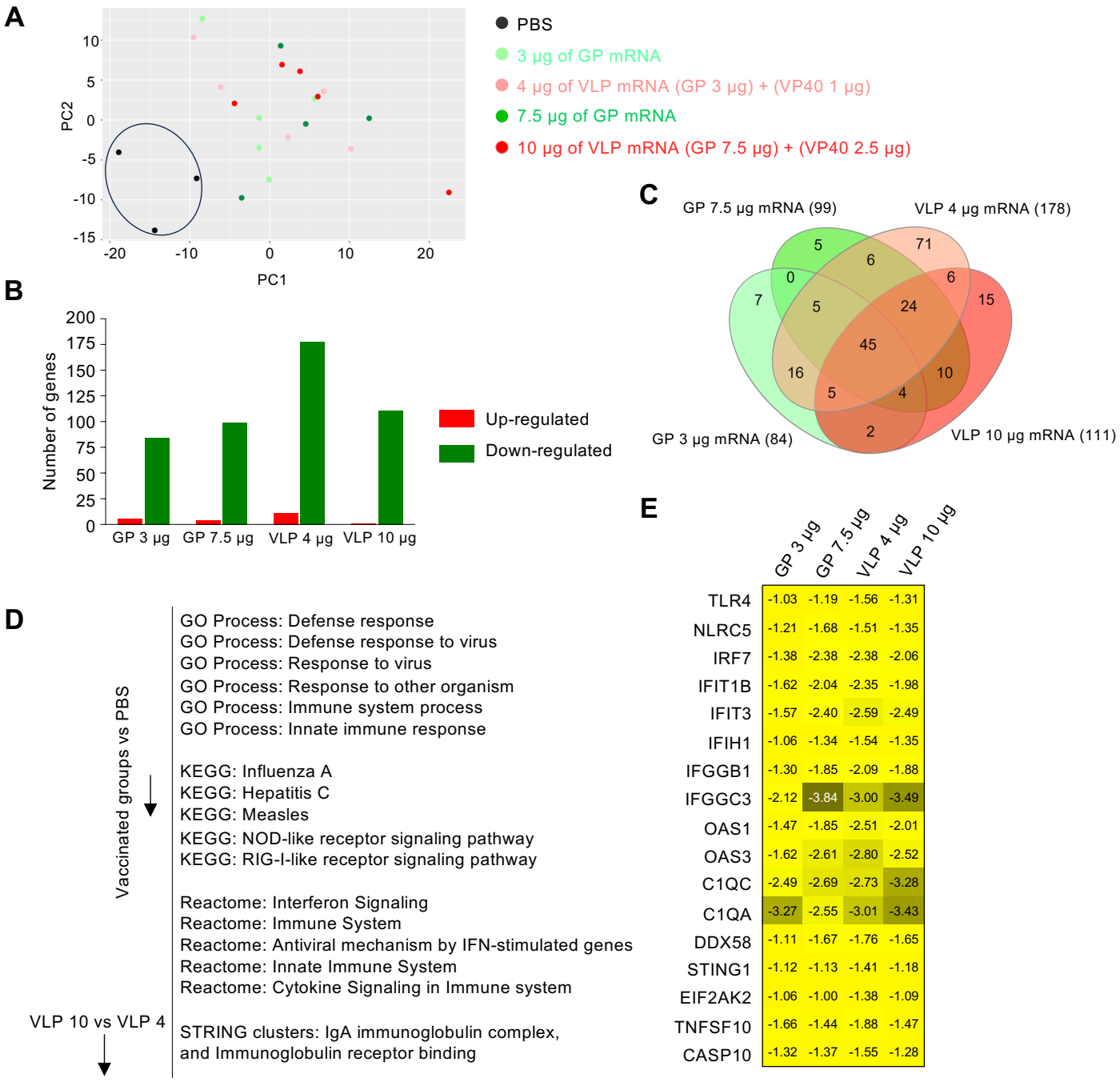

Figure 11. Vaccinated guinea pig groups show reduced expression of antiviral response genes compared to the unvaccinated group.

A. Principal component analysis (PCA) of genes expressed in control and vaccinated groups. The two outlier samples from the control group were removed for better visualization.

B. Total numbers of up and downregulated genes in the whole blood of vaccinated groups versus PBS. The graph shows genes with log2(fold change) ≥1 and adjusted p-vales of ≤ 0.05.

C. Venn diagram showing the intersection of overlapping downregulated genes among all vaccinated groups versus PBS.

D. Functional enrichment analysis of overlapping downregulated genes.

E. Genes related to immune response and apoptosis with log2(fold change) values.